Energy 313 (2024) 133706

Contents lists available at ScienceDirect

Energy

journal homepage: www.elsevier.com/locate/energy

Hybrid compressed air energy storage system and control strategy for a partially floating photovoltaic plant

Ameen M. Bassam [a], Nabil A.S. Elminshawy [b], Erkan Oterkus [c,*], Islam Amin [a,c]

[a] Department of Naval Architecture and Marine Engineering, Faculty of Engineering, Port Said University, Port Fouad, Egypt
[b] Department of Mechanical Power Engineering, Faculty of Engineering, Port Said University, Port Fouad, Egypt
[c] Department of Naval Architecture, Ocean and Marine Engineering, University of Strathclyde, Glasgow, UK

ARTICLE INFO

Keywords:
Compressed air energy storage
Energy management strategy
Rule-based approach
Photovoltaic systems
MATLAB
Simulink

ABSTRACT

For more efficient, reliable, and stable energy provision, energy storage plays a key role in the transition towards renewable energy sources. Compressed air energy storage (CAES) has been recognized as one of the most promising technology due to its high energy capacity, flexibility, scalability, long lifespan, maintainability, economical, and environmental viability. These potentials can be further improved by hybridizing CAES systems with thermal energy storage system. However, to realize the potentials of hybrid CAES systems, a control strategy is essential to manage the energy flow between the system components. Therefore, in this work, a novel energy management strategy is proposed to control a hybrid CAES system for a prototype of a partially floating photovoltaic plant (PFPV). The proposed control strategy is based on the rule-based approach and a mathematical model is presented to evaluate the system performance. The results indicate that, for an average hourly profile of the 5 kW PFPV platform through the year, a system round-trip efficiency of 34.1% can be obtained while the cycle and exergy efficiencies are 37.7% and 41%, respectively. Higher efficiency can be obtained by controlling the compressors operational range and rated power. Therefore, future work includes experimental work for results validation and optimization.

1. Introduction

With more than 80% of the global primary energy consumption is provided from fossil fuels, a sustainable and renewable energy transition is attracting widespread interest recently [1,2]. This interest is motivated by the continuously increasing economic growth, energy demand, environmental degradation, and the associated climate change threats. Therefore, many countries including Egypt have been triggered to increase the share of renewable energy in their energy mix for more secure, diverse and sustainable energy supply with lower greenhouse gas emissions [3]. For instance, a roadmap has been set by the Egyptian government, *Egypt's Vision 2030*, for the sustainable development and improving the share of renewable energy to 30% of the national energy mix by 2030 [4].

With a high solar energy abundance of 74 billion MWh/year, Egypt is considered as one of the most favorable environments for solar energy applications [5]. Among the variety of solar systems, photovoltaic (PV) systems are recognized as the most commonly utilized technology for power generation from solar energy [6]. This can be explained by the fact that PV systems are reliable, sustainable, modular, flexible, have quiet operation and long lifetime [7]. Therefore, numerous solar energy production projects in Egypt are operating or under construction deploying PV systems. The Egyptian government's efforts include large-scale solar PV projects (e.g. Benban solar park) as well as research and development projects to improve the performance of PV systems and overcome their challenges such as the working temperature rise of the PV panels, the high demand of open land area, and the intermittent fluctuated PV power supply.

For a sustainable and renewable green electricity supply to the rural areas around the Egyptian North Lakes, a novel partially floating PV (PFPV) concept has been proposed in [8]. In this concept, the PV modules are in a continuous and direct contact with the water body as shown in Fig. 1 which offers an efficient and costless passive cooling for the PV system. By controlling the ratio between the PV module submerged area ($A_{submerged}$) and the total PV surface area (A_{PV}), the PV system's operating temperature can be reduced which improves its performance and increases its output power [9]. Also, the proposed PFPV concept alleviates the looming land scarcity issue by implementing the PV system on the available water bodies such as lakes.

* Corresponding author.
E-mail address: erkan.oterkus@strath.ac.uk (E. Oterkus).

https://doi.org/10.1016/j.energy.2024.133706
Received 6 June 2024; Received in revised form 7 October 2024; Accepted 2 November 2024
Available online 16 November 2024

Abbreviations

A-CAES	Adiabatic compressed air energy storage
CAES	Compressed air energy storage
CE	Cycle efficiency
D-CAES	Diabatic compressed air energy storage
EMS	Energy management strategy
ESS	Energy storage system
EXE	Exergy efficiency
HP	High pressure
I-CAES	Isothermal compressed air energy storage
ID	Identity
LP	Low pressure
PFPV	Partially floating photovoltaic
PID	Proportional–integral–derivative
PV	Photovoltaic
RB	Rule-Based
RTE	Round-trip efficiency
SC-CAES	Supercritical compressed air energy storage
STIFA	Science, technology and innovation funding authority
TES	Thermal energy storage
UK	United Kingdom

Nomenclature

A_{PV}	Photovoltaic total area
$A_{submerged}$	Photovoltaic submerged area
C_P	Specific heat capacity
m	Mass
$\dot{m}$	Mass flow rate
P	Pressure
P_{C1}	First compressor power
P_{C1max}	First compressor maximum power
P_{C1min}	First compressor minimum power
P_{C2}	Second compressor power
P_{C2max}	Second compressor maximum power
P_{C2min}	Second compressor minimum power
P_{exp}	Expander power
P_H	Heater power
P_{Lo}	Required load power
P_{PV}	Photovoltaic power
Q_{air}	Heat addition to air
Q_h	Heater absorbed heat
Q_{water}	Heat addition to water
R	Air gas constant
T	Temperature
T_{cv}	Compressed air reservoir temperature
$T_{f,\ actual,\ comp}$	Compressed air actual final temperature
$T_{f,\ actual,\ exp}$	Expanded air actual final temperature
V	Volume of compressed air tanks
$\dot{W}_{actual,\ comp}$	Compressor actual power consumption
$\dot{W}_{actual,\ exp}$	Expander actual power generation
W_{ov}	Compressed air contained energy
β	Power distribution ratio
ε	Heat exchanger effectiveness
η_h	Heater electric efficiency
$\eta_{isen,\ comp}$	Compressor isentropic efficiency
$\eta_{isen,\ exp}$	Expander isentropic efficiency
γ	Air specific heat ratio
ΔE_{cv}	Air reservoir energy change
ΔT	Temperature difference

Subscript

cold	Cold fluid
f	Final
hot	Hot fluid
i	Initial
in	Inlet
out	Outlet

In order to overcome the solar PV intermittent supply, an energy storage system (ESS) can be used to store any excess energy during the day and use it later at night. Also, using an ESS not only solves the PV intermittency issue, but also improves the PV systems overall efficiency, reliability, stability, and their environmental and economic performance [10,11]. Among the available energy storage technologies for floating PV plants, compressed air energy storage (CAES) is one of the most promising systems [12]. This is due to the fact that CAES systems are reliable, flexible and durable systems with high energy density, power rating and long lifespan and discharge time compared with other energy storage technologies as can be observed in Fig. 2. Moreover, CAES systems have lower environmental impacts, require less maintenance, and can operate even in harsh environment conditions. These systems are also scalable from large scale to small and micro-scale systems which are portable and adaptable with grid-connected or stand-alone applications [12–14].

Due to these advantages, CAES systems have widely been investigated for the integration into renewable energy systems. For solar power applications, a techno-economic analysis has been performed in [17] for a CAES system integrated with a solar heliostat system and a desalination unit for the production of power and potable water showing a round trip efficiency of 48.7% and a payback period of only 2.65 year. In another study on solar heliostat systems, a higher round trip efficiency of 58.7% was reported in [18] by hybridizing the CAES system with a hydrogen storage system through recovering the waste heat of the solar unit to produce hydrogen. Also, CAES technology has been proposed for the integration with wind farms [19], hybrid wind and solar farms [20], hybrid solar and geothermal system [21], tidal turbine farms [22], and wave energy system [23]. Moreover, CAES technology can be combined with other renewable and alternative power systems such as biomass and biogas power systems [24,25], nuclear power plants [26], and fuel cell systems [27] which supports the high penetration of renewable energy. Furthermore, for emissions reduction, CAES has been proposed for carbon capture, utilization, and storage systems [28].

In CAES systems, surplus electric energy is converted into compressed air which is stored to be used later for electricity production by expanding the compressed air in a turbine generator [29]. According to the way of dealing with the heat generated during air compression, CAES systems can be classified into conventional diabatic, adiabatic, and isothermal systems [13]. In diabatic systems, the heat generated during air compression is wasted by cooling and an external energy source is utilized to heat the compressed air prior to the expansion process. This external heat source is normally provided by fossil fuels which reduces the energy efficiency and environmental performance of conventional diabatic CAES (D-CAES) systems [30]. On the other hand, adiabatic CAES (A-CAES) systems recover the heat generated during air compression and store it in a thermal energy storage (TES) system for heating the compressed air later during the discharge process. Consequently, adiabatic systems have higher efficiency and lower

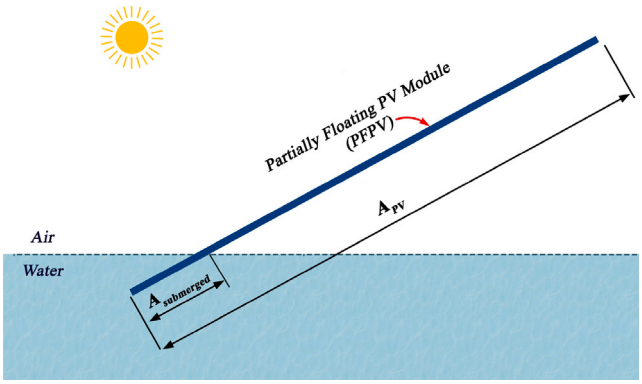

Fig. 1. Schematic diagram of the novel PFPV concept [8].

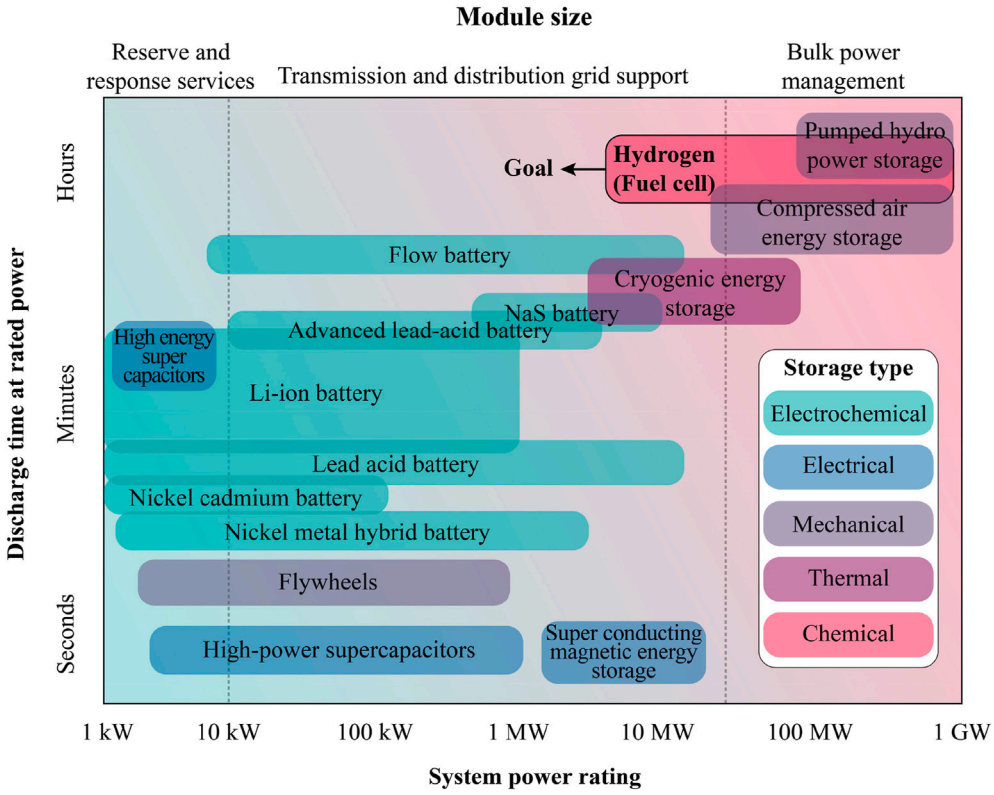

Fig. 2. Power rating and discharge time of different energy storage technologies [15,16].

emissions than diabatic systems. Meanwhile, isothermal CAES (I-CAES) systems have the lowest heat generation during air compression and air is stored near ambient temperature which reduces the required thermodynamic work and heat losses and improves the system efficiency [30]. However, adiabatic and isothermal CAES systems are more complex, difficult to achieve, and are not economically viable [30–32]. Also, there is no pilot or commercial plants that have been commissioned of A-CAES and I-CAES systems that have attained the expected performance and efficiency [30,33]. This is due to the fact that A-CAES and I-CAES systems require specialized machines and the available off-the-shelf equipment reduce the attainable performance and efficiency [13, 33].

Therefore, for the proposed novel PFPV plant in [8], a hybrid D-CAES system is proposed for the solar energy storage. The D-CAES concept is selected due to the maturity of its technology, the equipment availability, the successful demonstration of D-CAES systems in realistic conditions over several decades, and D-CAES systems have lower investment costs than A-CAES and I-CAES systems [30,32]. However, in order to overcome the disadvantages of D-CAES systems, a TES system is used to hybridize the D-CAES system for heating up the compressed air before its expansion in the turbine. The TES system utilizes a portion of the available solar power including the low-grade power which is not sufficient to operate the compressors of the CAES system. As a result, the proposed hybrid D-CAES has higher efficiency, fossil fuel independence, clean operation, and simple operation [34]. Also, in order to further improve the system's energy efficiency and reliability and overcome the solar energy intermittency issue, a multiple compressor system is used for the charging process in the CAES system. Accordingly, due to the presence of the CAES system with multiple compressors and the TES system together, an energy management strategy (EMS) is essential for the system operation and control.

The operating strategies and control of CAES systems have been previously discussed in the literature. The developed control strategy can deal with the CAES system on the system-scale, subsystem-scale, or on the components-scale. A simulation software tool has been developed for the modeling and control of A-CAES systems on the components,

subsystem, and the whole system level [31]. On the CAES system-scale, several control strategies have been developed for the economic optimization of CAES operation taking into consideration the electricity market prices [35,36]. Also, an EMS is required to deal with the intermittency nature of renewable energies and ascertain the economic feasibility of CAES as well. For example, a control strategy has been developed in [37] for a low-temperature A-CAES system integrated with wind power to ensure a stable power supply to the grid while maximizing the operation profitability. A control strategy has been also developed in [38] to minimize the associated costs of a microgrid with wind turbines, diesel generators, and an A-CAES system. Moreover, for a small-scale CAES system integrated with solar energy units and diesel generator, an EMS is proposed in [39] using linear programming for minimum operational cost, power loss, and emissions of the system. In [40], a control strategy with an objective of minimizing the daily operating cost of a hybrid power plant with a mini-CAES system, PV panels, and wind turbines has been developed using dynamic programming.

On the subsystem-scale control of CAES systems, an operating strategy can be developed to control a subsystem of the CAES system. For instance, the control of the discharge stage of CAES systems has been explored in several studies for better power tracking in grid applications. In [41], a feasible strategy to control the discharge stage of a grid-connected advanced A-CAES system has been proposed using a PID (Proportional–Integral–Derivative) controller. A state-space set-point control strategy is proposed in [42] to control the discharging process of a grid-scale advanced A-CAES system. In this strategy the power tracking is formulated as differential algebraic equations to control the turbine inlet pressure, air mass flow rate, and the fluid mass flow rate of the heat exchanger. Moreover, the performance of an advanced A-CAES tri-generative system can be improved by controlling the expanders' expansion ratio as investigated in [43]. The researchers in this study investigated the system discharge characteristics under different operating modes which improved the cycle efficiency from 39.32% to 40.55%. The same researchers reported a cycle efficiency of 48.31% in [44] for the same advanced A-CAES tri-generative system by controlling the operating pressure of the system compressors and expanders.

Some authors have also suggested a component-level control of CAES systems. For example, various control strategies have been proposed to adjust the expander inlet pressure to achieve the require power output [45]. For a tri-generative CAES system, a strategy has been proposed to independently control the turbine inlet pressure, air mass flow rate, or temperature while keeping the other two parameters constant [46]. A control strategy has been developed in [47] to control the compressor pressure, the water mass flow rate, and the flow rate of cryopump in a supercritical CAES (SC-CAES) system. A PID controller has been used in this control strategy for quicker load equilibrium with smaller load overshoot. Also, due to their simplicity, PID controllers have been proposed for the control of the compressor inlet guide vanes, air reservoir main valve, and circulating water pump in a CAES system with thermal storage [34]. Moreover, the control of the valves between the compressors and turbines has been proposed in [48] for an advanced A-CAES to change the series-parallel connection modes. Consequently, controlling the total pressure ratio of the compression and expansion processes can result in higher system efficiency.

From the above, it can be noticed that controlling CAES systems operation is a crucial issue for economic, environmental, and energy efficiency aspects. However, previous studies have almost exclusively focused on advanced CAES systems which includes A-CAES, advanced A-CAES, SC-CAES, and tri-generative CAES systems. Therefore, the objectives of this study include:

- Introduce a novel high-level supervisory control method for a hybrid CAES system which is proposed for the partially floating PV (PFPV) plant developed in [8] for electricity generation in rural areas around the Egyptian North Lakes. This strategy follows the deterministic Rule-Based approach to ensure a simple, robust, safe, and efficient operation of the hybrid CAES system while fulfilling the load requirements. This CAES system is diabatic and hybridized with a TES system for better performance and efficiency.
- Model the hybrid D-CAES-TES system and the proposed control strategy mathematically. The developed model is then validated, and implemented in MATLAB/Simulink environment to investigate the performance of the proposed system and control strategy. The performed study considers an average daily PV power profile for a year as well as a daily PV power profile per month.
- Perform a sensitivity analysis of the compressors' operational range as well as a sensitivity analysis of the compressors' rated power to investigate their impacts on the proposed hybrid CAES system performance and efficiency. The sensitivity analysis also includes varying the efficiency of the proposed CAES system's main components to have an indication of the system off-design performance.
- Investigate the environmental and economic benefits of the proposed hybrid CAES system compared with the conventional CAES system.

The rest of paper is organized as follow; Section 2 describes the developed PFPV prototype and the hybrid D-CAES. Section 3 introduces the proposed energy management strategy for the energy storage system. Section 4 illustrates the mathematical model of the hybrid D-CAES and control strategy while Section 5 presents the simulation implementation of these systems in MATLAB/Simulink with validation. Section 6 shows the simulation results and discussion. Finally, Section 7 presents the conclusions and future work.

2. System description

Towards a sustainable electric power generation for the rural coastal areas of Egypt, floating solar PV systems offer great potentials. The performance and potentials of a new concept of a floating PV system has been evaluated in [9]. In this concept, the PV system is partially submerged in the water for continuous and costless cooling and cleaning of the PV system as shown in Fig. 3. For the field-testing of this concept, a 10 × 10 m water basin with a depth of 1 m has been built for the testing at the campus of Port Said University, the Faculty of Engineering as shown in Fig. 4. According to the basin dimensions and the PV panel layout design, a 5 kW PFPV prototype model has been developed and introduced in [8].

The 5 kW pilot-scale system for this project was designed with a semisubmersible platform type as shown in Fig. 5. This is due to their stability, large deck area and payload capacity, cost-effectiveness, mobility, flexibility in the horizontal plane, and their limited sensitivity to the working water depth and mooring lines layout. Semisubmersible platforms are also scalable which allows the tailoring of the PV system capacity to meet the desired power output by selecting the suitable design and deck area of the platform. The main particulars of this platform are shown in Table 1. On top of this platform, 13 polycrystalline PV panels are mounted in 4 rows arrangement with a sufficient row spacing to avoid the adjacent PV modules shadowing.

Table 1
Principal particulars of the pilot-scale PFPV floating platform.

Parameter	Value
Length	8.6 m
Breadth	8.6 m
Depth	1.3 m
Draft	0.6 to 0.92 m
Weight	7 tons

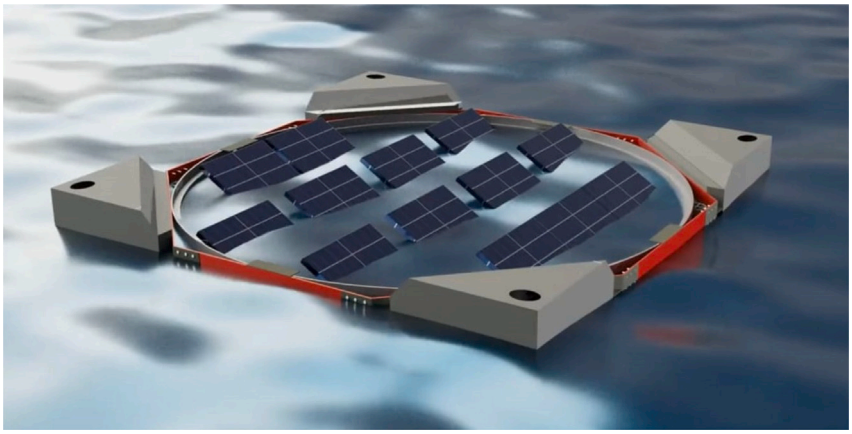

Fig. 3. Proposed partially submerged photovoltaic system.

Fig. 4. The partially submerged photovoltaic prototype platform in the water basin deployed at the campus of Port Said University, Egypt.

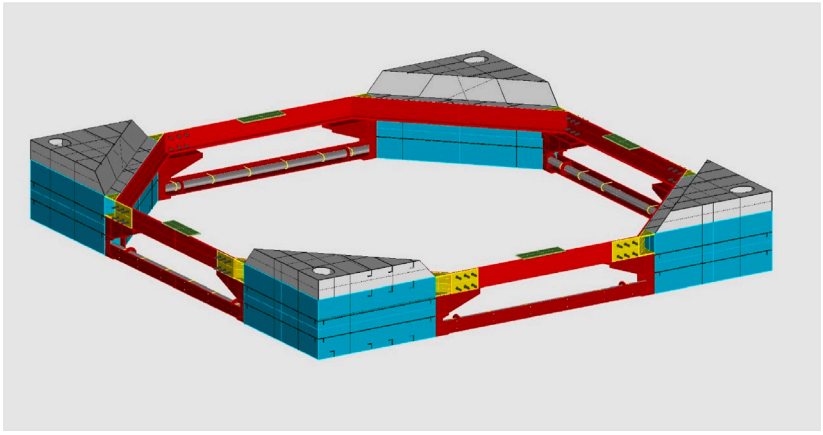

Fig. 5. Assembly and construction of the pilot-scale PFPV floating platform.

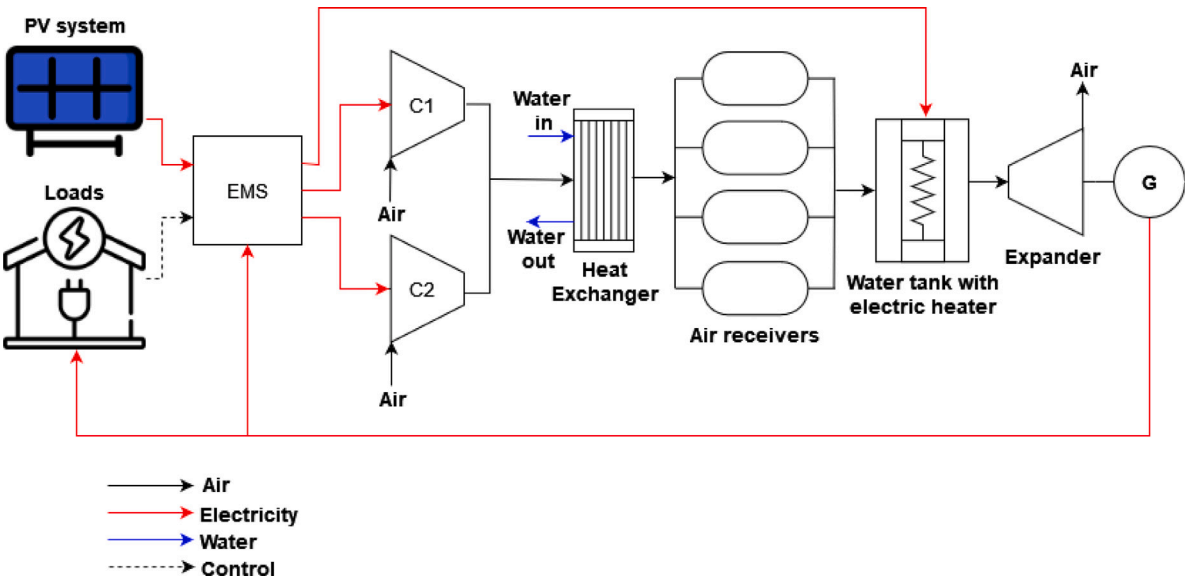

Fig. 6. Proposed hybrid energy storage system.

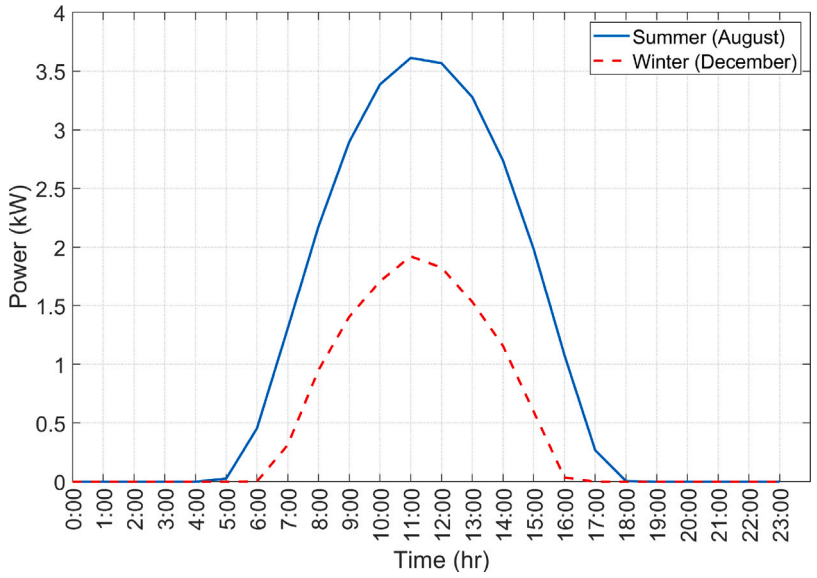

Fig. 7. Hourly profile of the PV power output of the 5 kW floating platform at Lake Bardawil, North Sinai, Egypt.

In order to address the PV power intermittency issue and provide a stable electricity supply throughout the day, a hybrid energy storage system is proposed as shown in Fig. 6. The main components of the system include compressors, heat exchanger, expander, air receivers, a water tank with an electric heater, and a generator.

Due to the variability of the 5 kW PV plant power production between winter and summer as shown in Fig. 7, multiple small variable speed air compressors are used in this project instead of a single compressor. As a result, less power is required for the compression start-up with better utilization of the available solar power as shown in Fig. 8. Moreover, compared with a single compressor operation, the proposed system has higher degree of operational flexibility, availability, reliability, and fault tolerance. Therefore, according to the available power from the proposed solar PFPV plant, two off-the-shelf industrial piston compressors with 1.5 kW rated power are selected.

Excess electricity from the PV system is used to compress air in the air storage system which consists of four uncompensated air steel tanks at the corners of the floating platform. Each tank has a constant volume of about 2 m^3 and an operating pressure of up to 30 bar. Prior to air storage, the hot compressed air is cooled down in the heat exchanger. Whenever the generated PV electricity is lower or higher than the required power by the air compressors, it is proposed to store this electricity in the form of heat in a TES. In this project, a hot water tank is used which is one of the most common heat storage technologies [49]. An electric resistance water heater is used to heat the water in the tank. Water is selected as a storage media because it is available, environmentally friendly, cheap, has a high heat capacity, and easy to store in insulated steel tanks [49]. The hot water tank is also integrated with a heat exchanger to raise the temperature of the compressed air prior to its expansion. Hence, the hot water tank in this system acts as a heat exchanger as well as a TES which stores part of the available PV electricity. As a result, there is no need for burning fossil fuels which improves the system efficiency and eliminates emissions. Then, during air discharge process, the compressed air is released and heated through the hot water tank before its expansion in the expander to regenerate electricity using the generator.

In order to manage the proposed ESS and properly split the available PV power between the load demands and the different components of

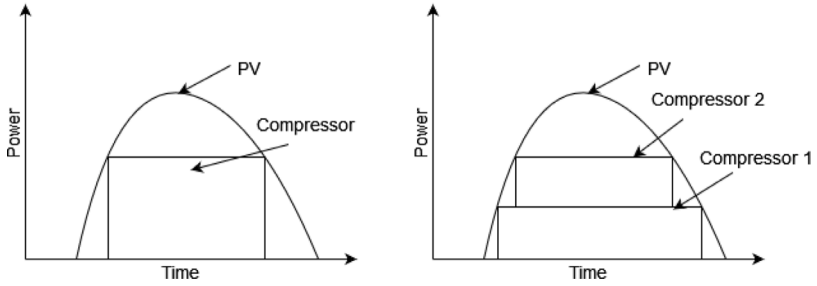

Fig. 8. Multiple compressors operation compared to single compressor operation.

the ESS, a suitable energy management strategy is required. This strategy controls the dynamic performance of the system and its components which influences the system's efficiency, feasibility, safe operation, and lifetime. In the following section, the developed EMS is described.

3. Energy management strategy

The proposed EMS in this project is based on the deterministic Rule-Based (RB) approach which is a high level supervisory control system. The RB approach is selected due to its simplicity, effectiveness, robustness, flexibility, and strong real-time performance [50,51]. This approach utilizes the human expertise, intuition, heuristics, and mathematical models to generate a set of predetermined rules which control the operation of the system components. These rules are interpretable and can be tuned for better performance of different operational scenarios with low computational burdens. Therefore, this approach is suitable for real-time controllers.

The main objectives of the developed strategy include fulfilling the load requirements at all time, splitting the available power efficiently between different components of the system, and reducing any power loss by utilizing even the low-grade PV power to improve the overall efficiency of the system. Moreover, the EMS objectives include ensuring the safe operation of the system components without exceeding their allowable operational limits. Consequently, the proposed strategy is developed based on the load requirements, the available PV power, the size and number of the CAES system's different components.

As shown in Fig. 9, the available PV power P_{PV} is always compared with the required load P_{Lo}. If the P_{PV} is lower than the P_{Lo}, the PV system cannot satisfy the load alone and the controller decides the required power from the expander P_{exp}. When the PV system is capable of satisfying the P_{Lo}, the surplus PV power is compared with the minimum power limit of the compressor. If the P_{PV} is lower than the P_{Lo} plus the minimum power of the first compressor P_{C1min}, the PV system supplies the load and the surplus PV power is stored in the TES system through the heater P_H. Meanwhile, the two compressors and the expander are not working. If the P_{PV} is higher than the P_{Lo} plus the minimum power of the first compressor P_{C1min}, the PV system supplies the load and operates the first compressor to compress air in the tank. Meanwhile, the second compressors, the heater, and the expander are not working. When the surplus PV power exceeds the maximum power of the first compressor P_{C1max}, the surplus power is compared with the minimum power required to operate the two compressors (P_{C1min}+P_{C2min}). If the surplus PV power is not sufficient to operate the two compressors at their minimum power, this surplus PV power operates the first compressor at the maximum power and the remaining power is stored in the TES system. If the surplus PV power is higher than the minimum power required to operate both compressors, the heater is shutdown and the PV power is split between the two compressors after satisfying the required load. When the PV system operates with maximum power, the two compressors operate at their maximum power and the remaining power is stored in the TES system after satisfying the required load.

4. Mathematical model

To store any excess PV power in the form of compressed air, the air pressure is increased from the atmospheric pressure to the storage pressure using compressors. Assuming steady state conditions and an ideal gas behavior of the air with constant mass flow rate and negligible potential and kinetic energy of the air, the actual power consumption of the compressor $\dot{W}_{\text{actual, comp}}$ can be determined as follow [52,53]:

$$\dot{W}_{\text{actual, comp}} = \dot{m}\,\frac{\gamma\, R\, T_i}{(\gamma-1)\,\eta_{\text{isen, comp}}}\left[\left(\frac{P_f}{P_i}\right)^{\frac{\gamma-1}{\gamma}} - 1\right] \tag{1}$$

where $\dot{m}$ is the air mass flow rate, γ is the air specific heat ratio, R is the air gas constant, T_i and P_i are the initial temperature and pressure of the air, respectively, P_f is the final air pressure, and $\eta_{\text{isen, comp}}$ is the isentropic efficiency of the compressor. The actual final temperature of air after compression $T_{\text{f, actual, comp}}$ is calculated by Mozayeni et al. [52]:

$$T_{\text{f, actual, comp}} = T_{\text{i}}\left[1 + \frac{1}{\eta_{\text{isen, comp}}}\left(\left(\frac{P_f}{P_i}\right)^{\frac{\gamma-1}{\gamma}} - 1\right)\right] \tag{2}$$

After compressing the air, a heat exchanger is used to cool the compressed air which increases its density. This heat exchanger utilizes the water body around the floating PV platform for cooling down the high-temperature compressed air. The effectiveness of the heat exchange process can be evaluated by ε as follows [53,54]:

$$\varepsilon = \frac{(\dot{m}\, C_P\, \Delta T)_{\text{cold or hot}}}{(\dot{m}\, C_P)_{\min}\,(T_{\text{hot, in}} - T_{\text{cold, in}})} \tag{3}$$

where $(\dot{m}\, C_P)_{\min}$ is the smaller of thermal capacity between the hot water and cold air streams. Since the heat capacity rate of the hot compressed air is smaller than the cold water, Eq. (3) can be rewritten as follows [53]:

$$\varepsilon = \frac{T_{\text{air, in}} - T_{\text{air, out}}}{T_{\text{air, in}} - T_{\text{water, in}}} \tag{4}$$

The compressed air is then stored in the platform corner tanks which are uncompensated and have a constant volume of V. The air pressure P change rate during charging and discharging can be calculated as follow [40]:

$$\frac{dP}{dt} = \frac{\gamma\, R}{V}(\dot{m}_{\text{in}}\, T_{\text{in}} - \dot{m}_{\text{out}}\, T_{\text{cv}}) \tag{5}$$

where $\dot{m}_{\text{in}}$ and T_{in} are the mass flow rate and temperature of the inlet air to the compressed air storage tank from the compressors while $\dot{m}_{\text{out}}$ is the outlet air mass flow rate to the expander from the compressed air storage tank. The temperature change rate of the compressed air reservoir T_{cv} can also be calculated as follows [52]:

$$\frac{dT_{\text{cv}}}{dt} = \frac{1}{m}\left(\dot{m}_{\text{in}}\, T_{\text{in}}\, \gamma + \left[(1-\gamma)\dot{m}_{\text{out}} - \dot{m}_{\text{in}}\right] T_{\text{cv}}\right) \tag{6}$$

where it is assumed that there is no heat exchange between the compressed air reservoir and the surrounding environment [48].

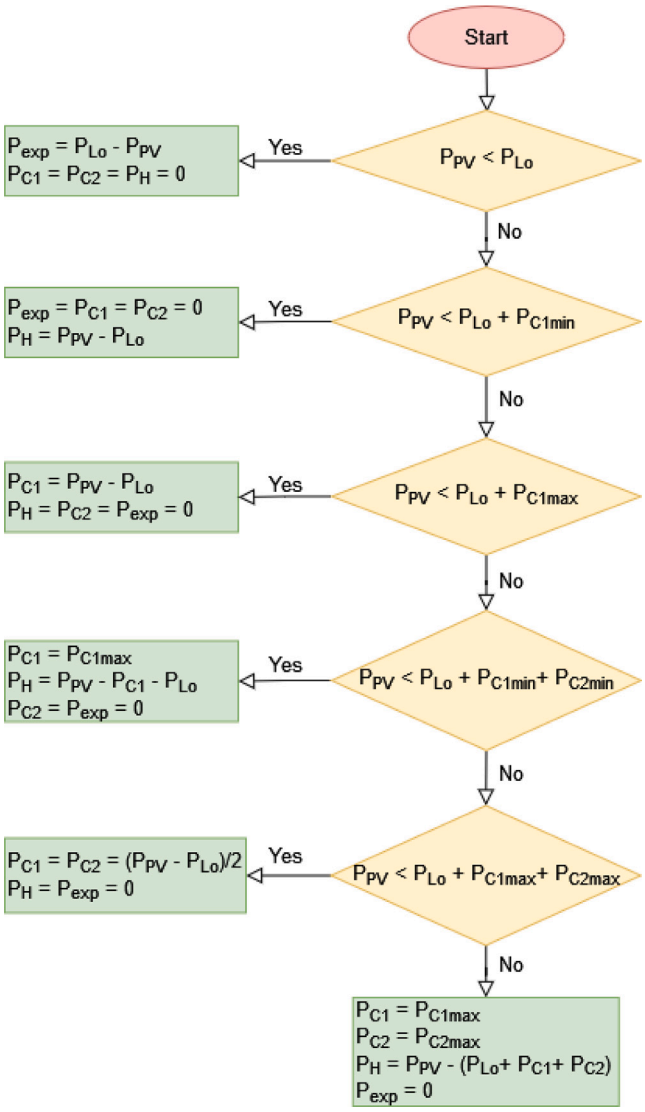

Fig. 9. Proposed rule-based EMS algorithm for the developed PFPV prototype.

The energy contained in the compressed air W_{ov} can be calculated as a function of the air storage tank volume V and the pressure inside and outside the tank P_{in} and P_{out}, respectively, as follows [55]:

$$W_{ov} = \frac{\gamma}{\gamma - 1} V P_{in}\left[1 - \left(\frac{P_{out}}{P_{in}}\right)^{\frac{\gamma-1}{\gamma}}\right] \tag{7}$$

In order to satisfy the required users electrical load, the compressed air energy can be extracted again by expanding the pressurized air through an expander and connect an electric generator to the expander shaft. The actual power generation from the expander $\dot{W}_{\text{actual, exp}}$ can be calculated as follows [52,53]:

$$\dot{W}_{\text{actual, exp}} = \eta_{\text{isen, exp}}\, \dot{m}\, \frac{\gamma R T_i}{\gamma - 1}\left[1 - \left(\frac{P_f}{P_i}\right)^{\frac{\gamma-1}{\gamma}}\right] \tag{8}$$

where $\eta_{\text{isen, exp}}$ is the isentropic efficiency of the expander. The actual final temperature of air after expansion $T_{\text{f, actual, exp}}$ can also be calculated by Wang et al. [53]:

$$T_{\text{f, actual, exp}} = T_{\text{i}}\left[1 - \eta_{\text{isen, exp}}\left(1 - \left(\frac{P_f}{P_i}\right)^{\frac{\gamma-1}{\gamma}}\right)\right] \tag{9}$$

Prior to the expansion process and in order to heat the air before the expander, the compressed air passes through the TES system acting as a heat exchanger. The heat exchanger effectiveness in Eq. (3) can be calculated as follows because the thermal capacity rate of air is smaller than the hot water thermal capacity [53,54].

$$\varepsilon = \frac{T_{\text{air, out}} - T_{\text{air, in}}}{T_{\text{water, in}} - T_{\text{air, in}}} \tag{10}$$

Then, by using the energy conservation law and neglecting any heat losses to the environment or pressure drop in the heat exchanger, the energy balance between the hot and cold fluids can be made to calculate the final temperature of water and the outlet temperature of the air as follows [54]:

$$m_{\text{water}}\, C_{\text{P, water}}\,(T_{\text{water, in}} - T_{\text{water, out}}) = m_{\text{air}}\, C_{\text{P, air}}\,(T_{\text{air, out}} - T_{\text{air, in}}) \tag{11}$$

The water in the TES is heated by an electric resistance heating system which converts part of the PV power into heat. The water temperature increase can be determined as a function of the absorbed heat Q_h as follows [56]:

$$Q_h = m_{\text{water}}\, C_{\text{P, water}}\,(T_{\text{water, out}} - T_{\text{water, in}}) \tag{12}$$

where m_{water} and $C_{\text{P, water}}$ are the water mass and specific heat at constant pressure, respectively. The required power by the heater P_H to supply Q_h can be calculated as a function of the electric heater efficiency η_h as follows [56]:

$$P_H = Q_h/\eta_h \tag{13}$$

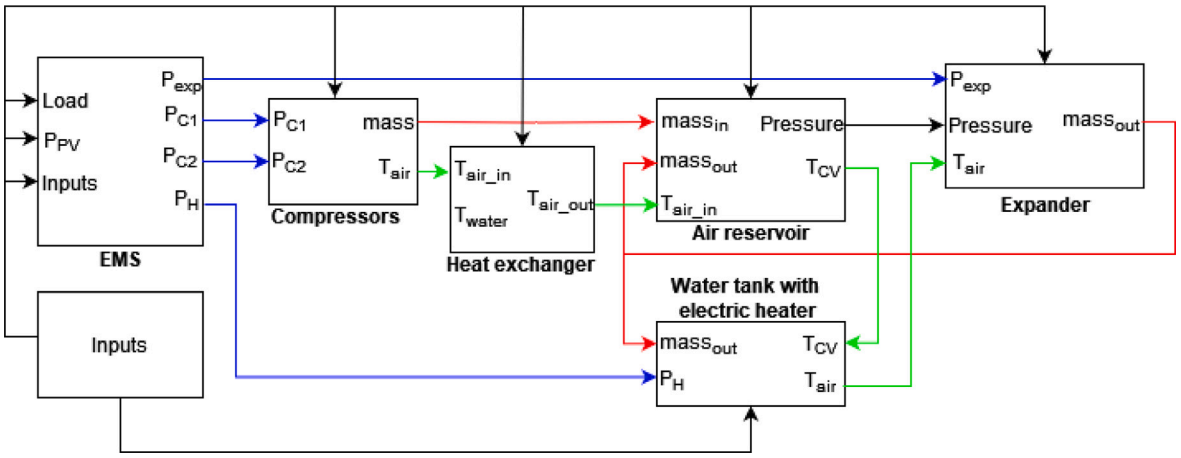

Fig. 10. Representation of the developed mathematical model of the proposed ESS in Simulink/MATLAB environment with the main inputs and outputs.

As explained earlier, part of the heat addition to water by the electric heater Q_h is used to heat the air before expansion Q_{air}. Another part of Q_h remains in the water Q_{water} which results in an increase in the water temperature inside the water tank. Therefore, Q_h is the sum of Q_{air} and Q_{water}.

In addition to fulfilling the load requirements, the developed control strategy distributes the available PV power between the CAES and TES systems as explained in the previous section. The power distribution ratio β can be defined as the ratio between the compression energy to the total input energy of compression and heat as follows [57]:

$$\beta = \frac{\int \dot{W}_{\text{actual, comp}}}{\int \dot{W}_{\text{actual, comp}} + \int P_H} \tag{14}$$

In order to evaluate the performance of the proposed ESS and control strategy, different performance indices can be used which include the cycle efficiency (CE) that can be defined as the ratio between the expansion energy and the compression energy as follows [44]:

$$CE = \frac{\int \dot{W}_{\text{actual, exp}}}{\int \dot{W}_{\text{actual, comp}}} \tag{15}$$

The round-trip efficiency (RTE) of the system can also be used to evaluate the system performance which is the ratio between the expansion energy and the total energy consumption of the compressor and the heat addition by the heater to the air Q_{air} as follows [57]:

$$RTE = \frac{\int \dot{W}_{\text{actual, exp}}}{\int \dot{W}_{\text{actual, comp}} + \int Q_{air}} \tag{16}$$

In order to include the exergy changes in the air reservoir and the water tank, an exergy efficiency (EXE) can be defined as follows [34,46]:

$$EXE = \frac{\int \dot{W}_{\text{actual, exp}} + Q_{water}}{\int \dot{W}_{\text{actual, comp}} + \int Q_{air} + \Delta E_{cv}} \tag{17}$$

where ΔE_{cv} denotes the energy change in the air reservoir which can be calculated according to Eq. (7) as a function of the initial and final pressures of the air reservoir.

5. Simulation implementation & validation

In order to study and evaluate their performance, the developed mathematical model of the proposed hybrid energy storage system illustrated in Fig. 6 as well as the control strategy are implemented in Simulink/MATLAB environment. As shown in Fig. 10, according to the load requirements and the available PV power, the EMS subsystem splits the available power between the compressors and the heater. In case of the available PV power is less than the required electrical load, the EMS subsystem requires power from the expander. The compressors subsystem receives the available power from the EMS subsystem and calculates the air mass flow rate according to Eq. (1) which is compressed and stored in the air reservoir. Before entering the air reservoir, the compressed air is cooled in the heat exchanger and the compressed air temperature after this cooling is calculated according to Eq. (4) in the heat exchanger subsystem. The air mass flow rate into and out of the air reservoir are balanced with the air temperature to calculate the compressed air pressure and temperature according to Eqs. (5) and (6) in the air reservoir subsystem. The required air mass flow rate by the expander subsystem according to Eq. (8) is heated before its expansion in the water tank and the air temperature is calculated in the water tank subsystem as shown in Fig. 10.

After implementing the mathematical model of the ESS in Simulink/MATLAB environment, the Huntorf CAES power plant is used as a case study for validation. The Huntorf plant was the first commercial D-CAES plant in the world commissioned in 1978 with a 290 MW output power and it was upgraded to 321 MW in 2006. The main components of this plant include a low-pressure (LP) compressor, a high-pressure (HP) compressor with 3 intercoolers, generator/motor, air cavern, LP and HP turbines [58]. For the retrofitted Huntorf plant, the simulated thermodynamical conditions of each components of the plant has been on-design assessed as explained in [59]. This on-design assessment has been used to calculate the power consumption and output of the retrofitted Huntorf plant's components. This data is used to validate the compressors and expander subsystems of the developed Simulink model in this study.

Table 2 provides the on-design operating conditions & parameters of the retrofitted Huntorf plant's components which are used as inputs to the developed Simulink model to validate the results of the compressors and expander subsystems. This data has been adapted from Jafarizadeh et al. [59].

As shown in Table 3, with an error of lower than 5%, there is a good agreement between the simulation results of the developed simulator in this study and the on-design calculations of the power consumption and output of the retrofitted Huntorf plant's components in [59]. In the following section, the developed Simulink model is used to evaluate the performance of the proposed ESS and control strategy.

6. Results

In this section, the performance of the proposed hybrid CAES-TES system in Fig. 6 integrating the control strategy in Fig. 9 is evaluated in terms of operational energy efficiency. The basic design parameters used for the simulations and their values are detailed in Table 4. Regarding the floating PV power plant, the system size is 5 kW with a PV tilt angle of 25° facing south as recommended for the application site which is Lake Bardawil, North Sinai, Egypt.

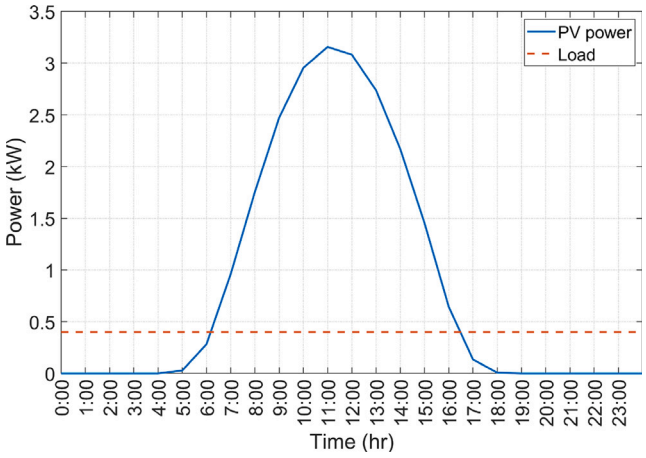

Fig. 11. Required load and the average hourly profile of the PV power output of the 5 kW floating platform at Lake Bardawil, North Sinai, Egypt.

Table 2
Operating conditions & parameters of the retrofitted Huntorf plant [59].

Parameter	On-design thermodynamic conditions
Compression air flow rate	108 kg/s
LP compressor isentropic efficiency	80%
LP compressor inlet pressure	101.325 kPa
LP compressor outlet pressure	540 kPa
LP compressor inlet temperature	15 °C
HP compressor isentropic efficiency	75%
HP compressor stage1 inlet pressure	535 kPa
HP compressor stage1 outlet pressure	1524 kPa
HP compressor stage1 inlet temperature	40 °C
HP compressor stage2 inlet pressure	1519 kPa
HP compressor stage2 outlet pressure	3025 kPa
HP compressor stage2 inlet temperature	59 °C
HP compressor stage3 inlet pressure	3020 kPa
HP compressor stage3 outlet pressure	5840 kPa
HP compressor stage3 inlet temperature	55 °C
Expansion air flow rate	432 kg/s
HP & LP turbine isentropic efficiency	86%
HP turbine inlet pressure	4200 kPa
HP turbine outlet pressure	1267 kPa
HP turbine inlet temperature	490 °C
LP turbine inlet pressure	1262 kPa
LP turbine outlet pressure	122 kPa
LP turbine inlet temperature	945 °C

6.1. Average daily PV profile

In order to study the performance of the proposed ESS and control strategy, an average hourly PV power output of the 5 kW plant is used. The average PV power profile shown in Fig. 11 is calculated for all months over a typical year according to Global Solar Atlas for the selected site [62]. For this analysis, the supplied local load has a daily energy demand of 9.6 kWh which is assumed to be flat during the day as shown in Fig. 11.

As shown in Fig. 12, the dynamic performance of the ESS is controlled according to the developed EMS. In the early morning hours when there is no or little solar power, the EMS imports the required load power from the electric generator as shown in Fig. 12(d). This electricity is produced by expanding the compressed air in an expander which reduces the air pressure in the air reservoir as shown in Fig. 12(e). Prior to the air expansion, the compressed air passes through the water electric heater tank to be heated which reduces the water temperature as shown in Fig. 12(f). Then, as the PV electricity generation increases, the load demand is supplied by the PV system and the required electricity from the electric generator decreases (4:00 to 6:00 a.m.) or stop which causes the air pressure to be constant between 6:00 to 8:00 a.m. During this time, the surplus electricity is not sufficient to operate the compressor. Therefore, the EMS operate the water electric heater to store the surplus PV power which increases the water temperature as shown in Fig. 12(f). When the surplus PV power exceeds the minimum required power to operate the first compressor (around 8:00 a.m.), the EMS stops the electric heater and operates the compressor until it reaches its maximum power as shown in Fig. 12(a). From 8:00 to 10:00 a.m., the surplus PV electricity is only sufficient to operate one compressor. Therefore, the EMS stores any excess power above the maximum power limit of the compressor in the TES system. When the PV system reaches the maximum generation value, the surplus electricity is sufficient to operate both compressors and the second compressor starts to work as shown in Fig. 12(b). Accordingly, the air pressure increases in the air reservoir. In the afternoon, the surplus PV power starts to decrease and the EMS operates one compressor plus the heater, or the compressor only, or the heater only according to the available PV power. By the evening, the generator starts to work again to supply the load demand.

For the studied hourly profile of the PV power and required load in Fig. 11, the EMS fulfills the required load and splits the surplus PV between the CAES and TES systems with a power distribution ratio β of 80.5%. The consumed compressor energy is 13.9 kWh while the absorbed heat energy by the TES is about 3.4 kWh. A part of this absorbed heat of 1.4 kWh is used to heat the air before its expansion while 1.6 kWh is absorbed by the water in the tank which raises its temperature as shown in Fig. 12(f). During the discharge, an energy of 5.24 kWh is produced from the expander which results in a cycle efficiency of 37.7%. By taking into consideration the added heat to air during expansion, the round-trip efficiency of the system is 34.1%. However, by taking into account the heat added to the exergy changes in the air reservoir and the water tank, the exergy efficiency is 41%.

6.2. Daily PV profile per month

For the selected application site, the daily average production of the 5 kW floating PV system can be obtained per month from the Global Solar Atlas [62]. As shown in Fig. 13, due to the PV power fluctuation over the year, the load requirement from the PV system varies from month to month. During summer months (May, June, July, and August), the daily required load is 13.2 kWh. While in spring and autumn months, the daily required load varies between 7.8 to 12 kWh. In winter months (January and December), the required load is 6 kWh when the PV system has a low electricity production.

The daily PV available energy and load requirement for each month shown in Fig. 13 as well as the data in Table 4 have been used as inputs to the Simulink model of the proposed ESS to evaluate its performance.

Table 3
Comparison of the on-design calculations and simulation results for the retrofitted Huntorf plant [59].

Parameter	On-design calculations	Simulation results	Error (%)
LP compressor output power	24.01 MW	23.94 MW	0.29
HP compressor1 output power	15.81 MW	15.78 MW	0.19
HP compressor2 output power	10.45 MW	10.45 MW	0
HP compressor3 output power	9.823 MW	9.837 MW	1.18
HP turbine output power	84 MW	82.56 MW	1.74
LP turbine output power	231.28 MW	221.4 MW	4.46

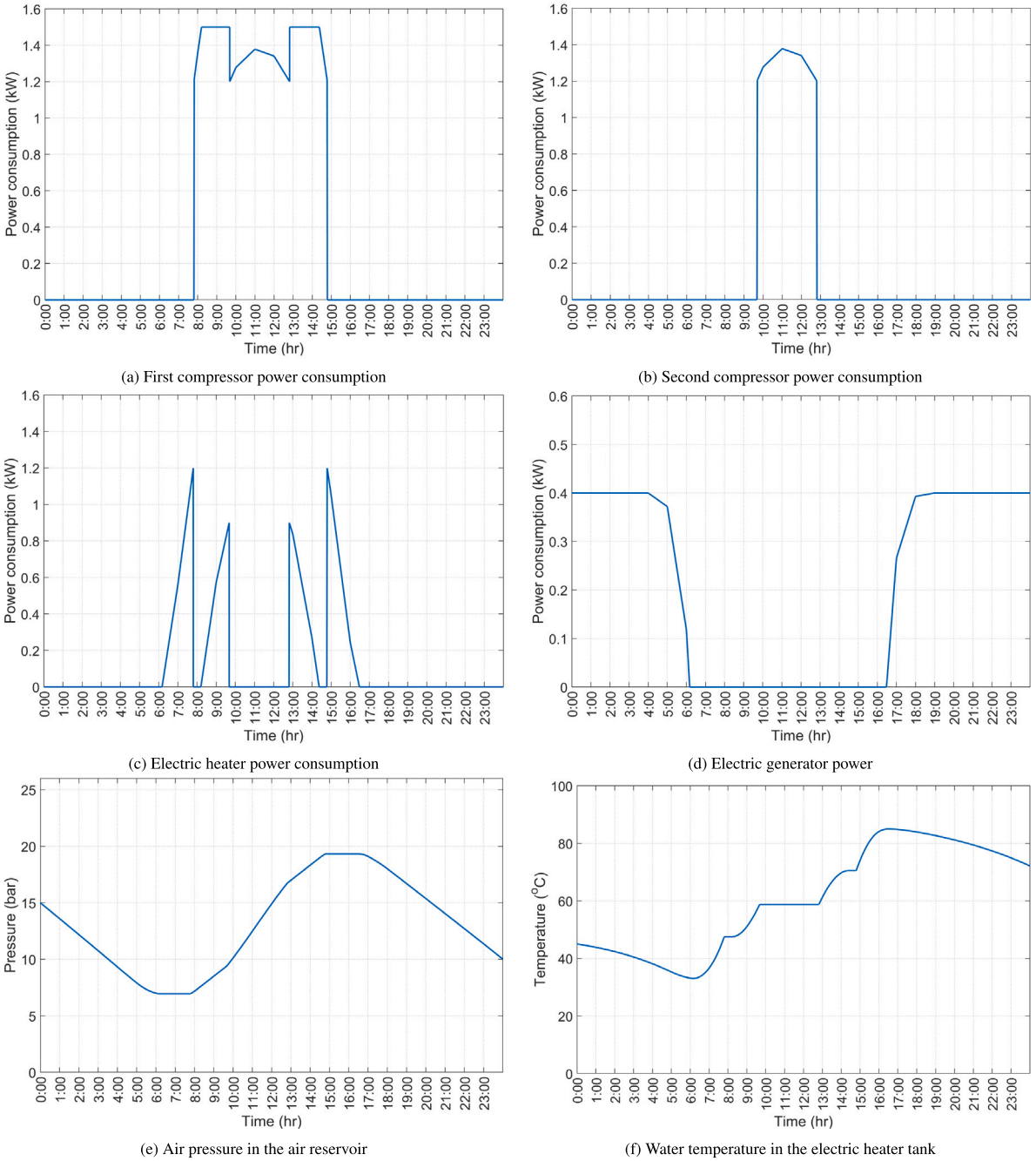

(a) First compressor power consumption
(b) Second compressor power consumption
(c) Electric heater power consumption
(d) Electric generator power
(e) Air pressure in the air reservoir
(f) Water temperature in the electric heater tank

Fig. 12. Simulation results of the proposed ESS system and control strategy based on an average daily PV profile.

According to the proposed control strategy, the available PV power is split between the required load and the energy storage system's components as shown in Table 5. The ratio of power distribution between the CAES and TES systems β fluctuates between 83% to 86% most of the year except for the winter months of November, December, January and February. This is due to the fact that the PV

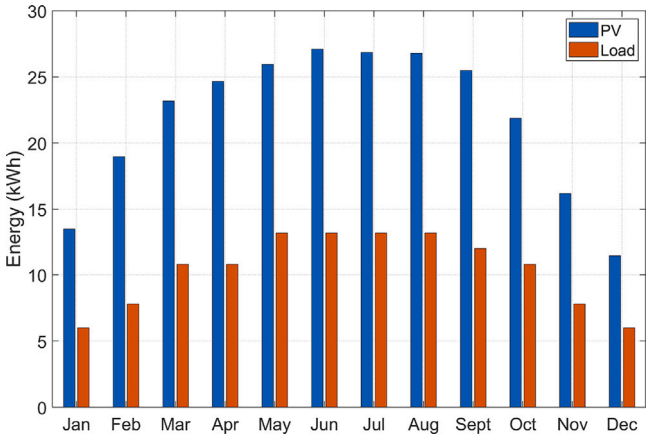

Fig. 13. Daily PV energy production of the 5 kW PV floating platform and load requirement per month.

Table 4
Design parameters of the proposed hybrid CAES-TES system.

Parameter	Value
Air specific heat ratio	1.4
Air gas constant	0.287 kJ/kg K
Inlet air temperature to compressors	21 °C
Inlet air pressure to compressors	1.013 bar
Outlet air pressure of compressors	30 bar
Compressors isentropic efficiency	87.5% [60]
Compressors rated power	1500 Watt
Compressors operational limits	80% to 100%
Expander isentropic efficiency	92.5% [60]
Air reservoirs volume	8 m^3
Air reservoirs operating pressure	up to 30 bar
Air reservoirs initial temperature	21 °C
Air specific heat	1 kJ/kg K
Water tank volume	50 liter
Water initial temperature in the heater tank	45 °C
Water inlet temperature to the heat exchanger	25 °C
Water specific heat	4.2 kJ/kg K
Heat exchanger efficiency	90% [53]
Electric heater efficiency	90% [61]

system output decreases in winter which is not sufficient to operate the two compressors of the CAES system. Therefore, the EMS stores more energy in the TES system which reduces the power distribution ratio β.

Fig. 14 compares the daily performance of the proposed ESS and control strategy in two typical days in summer (June) and winter (December). As mentioned earlier, less PV power is available in winter making it insufficient to power the second compressor of the CAES system as shown in Fig. 14(b). As a result, higher energy percentage is supplied to the heater as shown in Fig. 14(c) which increases the water temperature in the water tank in winter compared to summer as shown in Fig. 14(f). On the other hand, more PV power is available in summer and the ESS can fulfill higher load as shown in Fig. 14(d). Also, more power is available for the compressors which will work more in summer than winter as can be seen in Figs. 14(a) and 14(b). Consequently, higher air pressure can be reached as shown in Fig. 14(e) which does not exceed the safety limits of the system.

These results suggest that the proposed system in this work can be used for power and heat supply especially in winter. This is because higher percentage of the available PV power is stored as heat in the water tank in winter. Consequently, higher efficiency can be attained by the proposed system by supplying heat and power.

Regarding the efficiency of the proposed system, it is significantly affected by the power distribution ratio between the CAES and TES systems β. As shown in Fig. 15, at lower β values, higher system efficiency can be obtained. This is due to the fact that lower energy percentage is stored in the CAES system at lower β values which reduces the compression losses and increases the system efficiency. The system higher efficiency in winter months of November, December, and January is also associated with the low load requirements and power consumption of the compressors and expander as can be seen in Fig. 13 and Table 5.

As illustrated by Fig. 15, the system's cycle efficiency fluctuates between 38% and 45% except for winter months when CE is about 65% in December. The round trip efficiency of the system also varies from about 33% to 40% except for December when an RTE of 53% can be achieved. Regarding the exergy efficiency, it ranges from 33% to 48% between February and November with a highest EXE of 64% in January.

Table 6 compares the efficiency of the proposed hybrid CAES system in this study to similar systems in terms of size or configuration. Compared with small and micro-scale CAES systems, results show that the proposed system has superior performance in terms of efficiency. The results also show that the proposed system has comparable efficiency with advanced CAES system such as A-CAES and advanced A-CAES or hybrid TES-CAES of larger scale as shown in Table 6.

6.3. Sensitivity analysis

6.3.1. Compressor operational range

To this point, the reported performance results of the ESS are based on an operational range of the variable speed compressor from 80% to 100% as shown in Table 4. With a maximum power of 100%, a variable speed compressor can operate with a minimum power of up to 20%. However, for more efficient operation, higher reliability, and less overheating, the compressor loading is around 80% as recommended by the manufacturers. In order to study the sensitivity of the system performance to the compressor loading operational limits, different minimum power values of the compressor are used by the proposed control strategy for the simulation of the proposed hybrid ESS considering the average PV power profile as shown in Fig. 11.

As shown in Fig. 16, the compressor minimum loading threshold affects the power distribution ratio between the CAES and TES significantly. By lowering the compressor minimum loading threshold to 75%, more PV power will be utilized by the compressors according to the control EMS as shown in Figs. 16(a) and 16(b). This is mainly due to the fact that the compressors will have more operational time by lowering their minimum loading threshold. For example, the second compressor operates for about 4 h when the compressor minimum loading threshold is 75% compared to 2 operational hours when the compressor minimum loading threshold is 85% as shown in Fig. 16(b). As a result, higher air pressure can be obtained in the air reservoir when the compressor minimum loading threshold is 75% as can be seen in Fig. 16(e).

Table 5
Daily energy consumption of the proposed energy storage system's components and power distribution ratio for each month.

Month	Compression energy (kWh)	TES energy (kWh)	β(%)	Expander energy (kWh)	Q_{air} (kWh)	Q_{water} (kWh)	ΔE_{cv} (kWh)
January	6.85	4.19	62.0	3.68	1.29	2.48	1.49
February	12.30	3.31	78.8	4.63	1.27	1.71	1.08
March	15.26	2.98	83.7	6.11	1.75	0.93	2.05
April	16.40	3.07	84.2	5.83	1.49	1.27	1.28
May	16.31	3.12	83.9	6.95	2.23	0.58	3.06
June	17.44	3.01	85.3	6.83	1.95	0.76	2.35
July	17.23	3.05	85.0	6.89	2.05	0.69	2.61
August	17.47	2.91	85.7	7.09	2.16	0.46	2.98
September	17.12	2.77	86.1	6.67	1.83	0.67	2.23
October	14.30	2.93	83.0	6.40	2.03	0.60	2.84
November	9.50	3.53	72.9	4.83	1.64	1.53	2.08
December	5.81	3.25	64.1	3.77	1.33	1.60	1.96

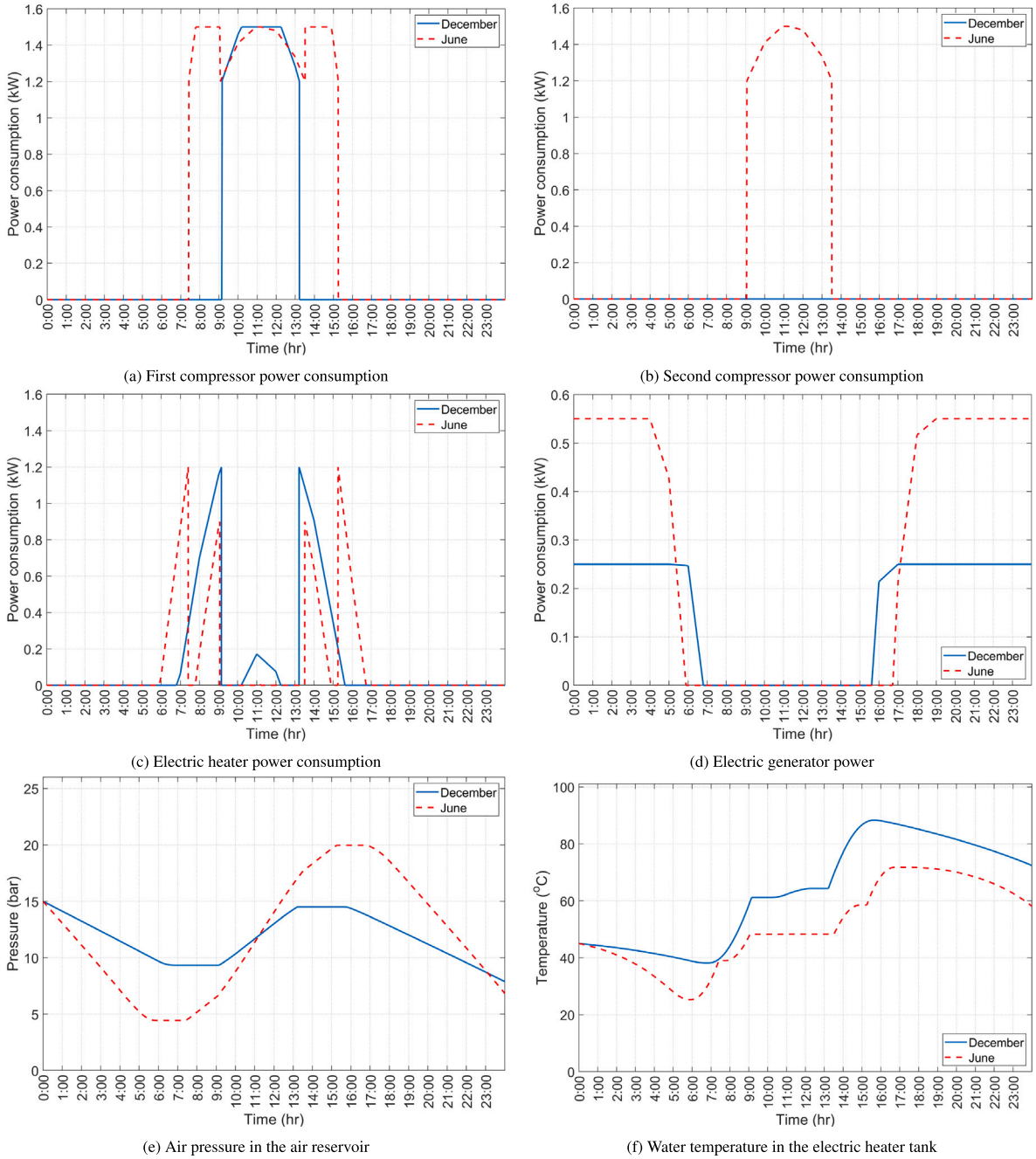

(a) First compressor power consumption
(b) Second compressor power consumption
(c) Electric heater power consumption
(d) Electric generator power
(e) Air pressure in the air reservoir
(f) Water temperature in the electric heater tank

Fig. 14. Simulation results of the proposed ESS system and control strategy daily performance for the months of June and December.

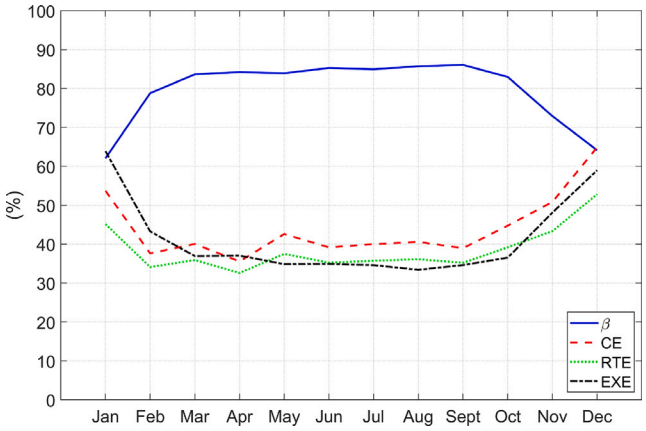

Fig. 15. Monthly power distribution ratio and efficiency of the proposed hybrid CAES system.

Table 6
Comparative analysis of efficiency with previous studies.

Reference	System	Power	Efficiency
Current study	Hybrid TES-CAES	<1 kW	33–53%
[63]	CAES	<1 kW	23–36%
[64]	Tri-generative CAES	2 kW	15.6%
[56]	A-CAES	3.2 kW	13–25%
[65]	Advanced A-CAES	23.5 kW	33.7%
[66]	Hybrid TES-CAES	500 kW	22.6%
[67]	Hybrid TES-CAES	100 MW	24.5–57.5%
[32]	Hybrid TES-CAES	100 MW	53%

On the other hand, by increasing the compressor minimum loading threshold, the compressors will have less time to operate and the available PV power will be utilized by the electric heater according to the control EMS. Accordingly, as shown in Fig. 16(c), more power is consumed by the electric heater when the compressor minimum loading threshold is 85% which increases the water temperature inside the water tank as shown in Fig. 16(f). For both conditions, the system delivers the same required load as shown in Fig. 16(d). These results suggest that the compressor minimum loading threshold can be controlled according to the load requirement of electric power or heat or both power and heat in a cogeneration system.

Regarding the power distribution ratio and efficiency of the proposed system, by increasing the compressor minimum loading threshold, less power is utilized by the compressors which reduces β as shown in Fig. 17. As discussed earlier, more system efficiency can be obtained at lower β values. However, by increasing the compressor minimum loading threshold, more power is utilized by the TES system and less power is available for the compressors. Consequently, the water temperature may exceed the maximum allowed temperature and more compressed air will be withdrawn for the air reservoir by the end of the daily cycle.

As shown in Fig. 17, by increasing the compressors' minimum loading thresholds from 75% to 85%, the CE, RTE, and EXE can be improved by 4.8%, 3%, and 9.5%, respectively, by considering the average PV power profile as shown in Fig. 11.

6.3.2. Compressor rated power

As explained in Section 2, due to the solar energy variability, two variable speed compressors with a rated power of 1.5 kW are selected instead of a single compressor. In order to investigate the impact of this parameter on the performance of the hybrid D-CAES system, different compressor rated powers with a minimum loading threshold of 80% have been used by the proposed control strategy for the simulation considering the average PV power profile in Fig. 11.

As shown in Figs. 18(a) and 18(b), by increasing the compressors rated power, both compressors will have less running time considering the same PV power profile. Consequently, less air pressure will be obtained by the end of the day as shown in Fig. 18(e). Also, by increasing the compressors rated power, the proposed control strategy will store more energy in the TES system by the heater as shown in Fig. 18(c) which results in a rise in the water temperature in the tank as can be observed in Fig. 18(f).

Moreover, as shown in Fig. 19, by increasing the compressors rated power, lower β values and higher efficiency of the system can be obtained because less power will be utilized by the compressors which reduces the system losses. However, at lower β values, the reliance on the TES system is increased. Therefore, more water storage size will be required to allocate the increased amount of stored energy in the TES system. Otherwise, the proposed CAES system can be used to supply heat and power which utilizes the TES energy without increasing its size and improves the system overall efficiency.

As shown in Fig. 19, by increasing the compressors' rated powers from 1.4 kW to 1.6 kW, the CE, RTE, and EXE can be improved by 3.4%, 2.1%, and 6.8%, respectively, by considering the average PV power profile as shown in Fig. 11.

It should be noted that the reported efficiency results are based on the developed mathematical model and the made simplifications and assumptions. However, experimental work is the next step after completing the PFPV prototype build up to evaluate the hybrid CAES system, the proposed control strategy, and validate the mathematical model. Also, the effect of the power distribution ratio β on the system performance is noticeable as can be seen in Figs. 17 and 19. Therefore, future work should focus on optimizing the value of β and studying the possibility of supplying heat or recovering the heat and cold generated during the compressed air compression and expansion in a cogeneration or trigeneration system.

6.3.3. Efficiency of the compressor, expander & electric heater

Due to the variability of solar energy and environmental conditions or changes in the required loads, the components of CAES systems can operate under off-design conditions which affects their performance and the system's efficiency. Therefore, in order to have an indication

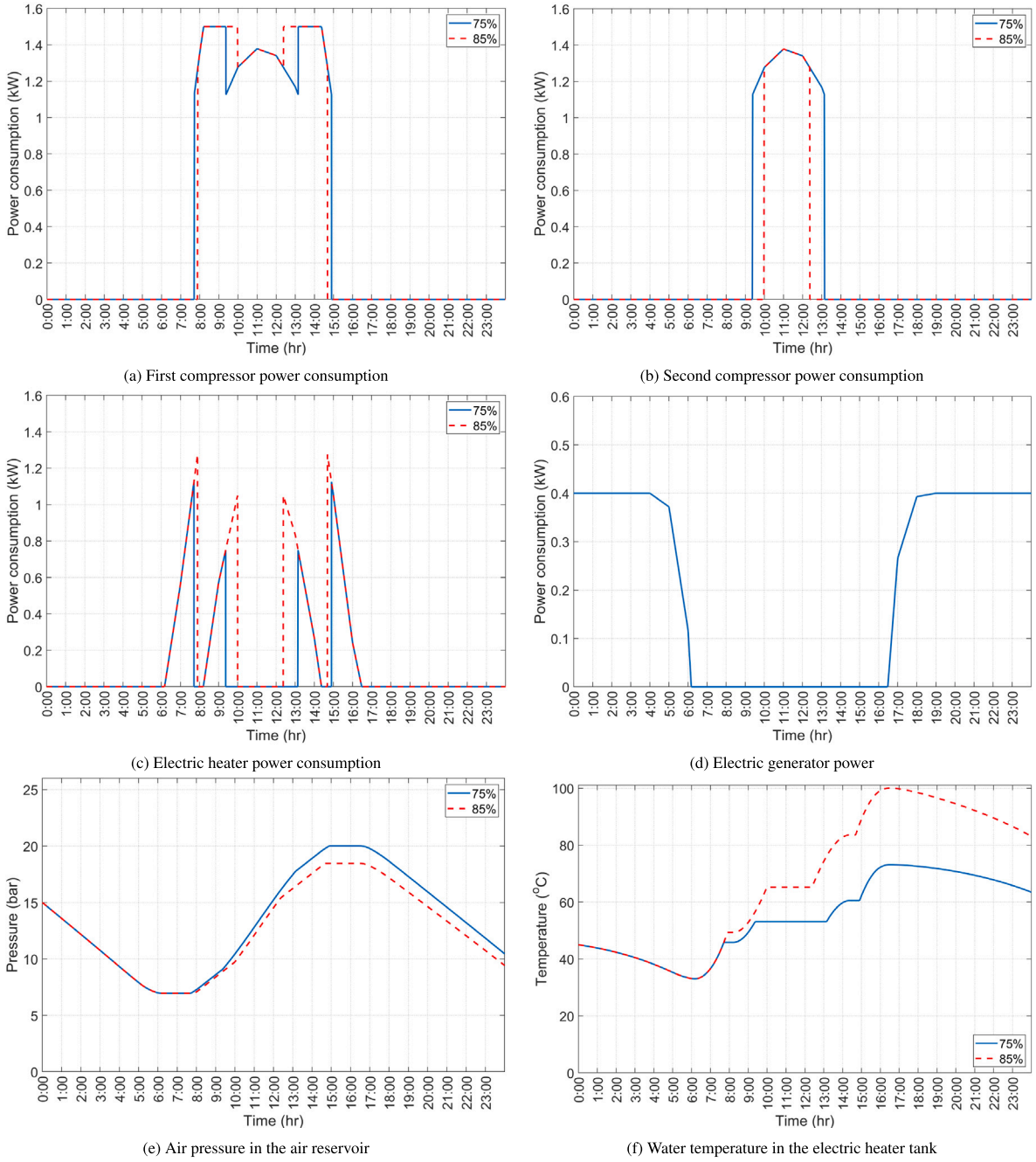

(a) First compressor power consumption

(b) Second compressor power consumption

(c) Electric heater power consumption

(d) Electric generator power

(e) Air pressure in the air reservoir

(f) Water temperature in the electric heater tank

Fig. 16. Simulation results of the proposed ESS system and control strategy based on an average daily PV profile.

about the off-design performance of the system, a sensitivity analysis is performed to investigate the effect of the efficiency of the CEAS system's main components which include the compressor, expander and electric heater.

Since the required load, PV power profile, and the compressors' rated power and operational range are the same for different scenarios, the power flow between the system components is the same according to the developed control EMS. As a result, the power distribution ratio β and the system's CE are the same for different values of the efficiency of the compressors, expander, and the electric heater as shown in Figs. 20 to 22.

As shown in Fig. 20, the system's EXE improves at higher isentropic efficiency of the compressor. This is due to the fact that higher stored energy and air pressure can be achieved in the air reservoir at higher compressor's isentropic efficiency. Consequently, the CAES system has less energy change in the air reservoir and higher EXE according to Eq. (17). Also, the system's RTE slightly improves at higher compressor's isentropic efficiency. This is because higher compressor's isentropic efficiency will result in higher air mass flow rate and less compression heat which has a marginal effect on the temperature change rate of the compressed air reservoir and consequently the heat addition by the heater to the air.

The effect of the expander's isentropic efficiency on the system performance can be also observed in Fig. 21. The results show that the RTE and EXE of the CAES system increases at higher expander's isentropic efficiency. This is because the higher the expander isentropic efficiency, the less mass flow of the expander is required. As a result, less heat addition by the heater to the expander air mass flow rate and higher heat addition by the heater to the water which improves the system's RTE and EXE.

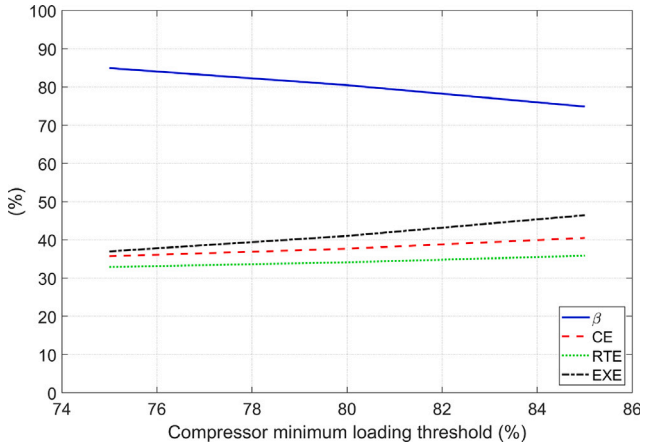

Fig. 17. System power distribution ratio and efficiency at different thresholds of the compressor minimum loading.

Table 7
Input parameters for the environmental & economic benefits analysis [46,68].

Parameter	Value
Natural gas calorific value	35 MJ/N m^3
Natural gas price	0.6 $/N m^3
Burner efficiency	90%
CO_2 emissions factor	55 kg/GJ

Fig. 22 shows the effect of the electric heater efficiency on the system performance. As the electric heater efficiency increases, the heat absorbed by the water in the water tank as well as the heat addition by the heater to the air increases. As a result, the system's EXE increases due to the increase in the water temperature inside the water tank and the system' RTE slightly decrease because more thermal energy is absorbed by the air during expansion.

6.4. Environmental & economic benefits

Compared with a conventional CAES system, the proposed system eliminates the need for burning fuel, typically natural gas, to raise the air temperature before the expansion process. Consequently, the proposed hybrid CAES system can save a fuel consumption of 126.4 m^3 of natural gas per year which is equivalent to the energy added to the TES and air before expansion considering the average daily PV profile in Section 6.1. Also, this fuel consumption could result in a CO_2 emissions of about 243.4 kg per year according to the data in Table 7.

This fuel saving will also result in an economic benefit by reducing the system operational cost by 27690 $/year of fuel cost. Moreover, the proposed novel PFPV concept has resulted in higher power production compared with the land-based PV system. The output power improvement can reach 20.76% according to the PV panels submergence ratio as reported in [9]. Accordingly, the CO_2 emissions and cost of electricity generated by the PFPV plant is lowered. Furthermore, a water tank with electric heater for the proposed hybrid CAES system is much cheaper than a combustion chamber for the conventional diabatic CAES system which further reduces the associated costs of the system. Therefore, a more detailed economic investigation is required for the novel PFPV concept integrated with the proposed hybrid CAES system to evaluate the economic feasibility and viability of the system with different submergence ratio of the PFPV system.

7. Conclusions

Towards a real energy transition to renewable energy sources, energy storage systems have a crucial role to play. In this study, a hybrid diabatic CAES-TES storage system has been proposed for a partially floating PV system to provide the rural areas around the Egyptian north lakes with electricity. Also, a novel deterministic rule-based EMS has been developed in this study to efficiently manage the power flow between the storage system different components. In order to investigate the energy storage system and EMS performance, a mathematical model has been developed in the MATLAB/Simulink environment and validated with the on-design operating conditions and parameters of the retrofitted Huntorf plant. The main conclusions of this paper can be summarized as follows:

- Simulation results show that the proposed novel EMS effectively fulfills the required load and manages the power split between different components of the ESS. For an average hourly profile of the PV power output of the 5 kW floating platform throughout the year, a system round-trip efficiency of 34.1% can be obtained while the cycle and exergy efficiencies are 37.7% and 41%, respectively.
- For an average hourly profile of the PV power output for each month, the RTE, CE, EXE of the proposed ESS fluctuate between 33% to 40%, 38% to 45%, and 33% to 48% between February and October, respectively. The highest system efficiency has been observed in January and December with values of 53%, 65%, and 64% for the system's RTE, CE, and EXE, respectively.
- Compared to conventional CAES systems, the proposed hybrid CAES system has an annual fuel saving of 126.4 m^3 of natural gas. Consequently, a CO_2 emissions saving of about 243.4 kg per year can be achieved. This fuel saving will also result in an economic benefit by reducing the system operational cost by 27690 $/year of fuel cost.
- The performed sensitivity analyses show that the selected compressors rated power and minimum loading threshold affect the system's performance and efficiency considerably. It has been shown that by increasing the selected compressors' rated power and minimum loading threshold, less power would be utilized by the CAES and more power would be utilized by the TES. Consequently, lower compression losses can be achieved which improves the ESS exergy and energy efficiencies. However, larger size of the TES system would be required to accommodate the available energy.
- The sensitivity analyses also show that the system's energy and exergy efficiency can be considerably affected by the components efficiency which can decrease under off-design and partial load operation conditions.

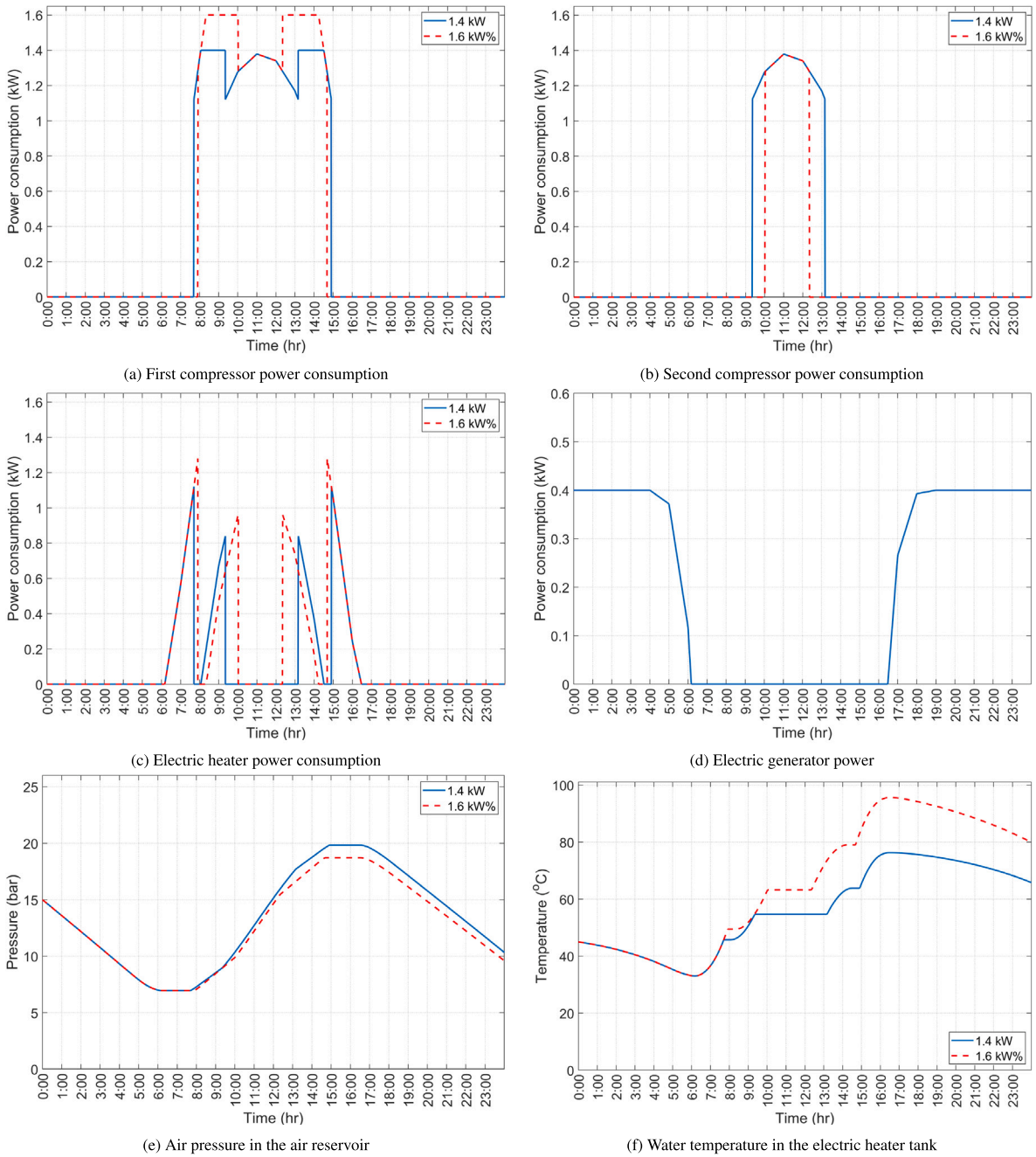

(a) First compressor power consumption

(b) Second compressor power consumption

(c) Electric heater power consumption

(d) Electric generator power

(e) Air pressure in the air reservoir

(f) Water temperature in the electric heater tank

Fig. 18. Simulation results of the proposed ESS system and control strategy based on an average daily PV profile.

7.1. Further work

Future work includes the completion of the PFPV prototype plant build up and starting the experimental work. This includes the mounting and orienting the PV panels on the floating platform, the built-up of the hybrid CAES system, hardware and software setup of installing the sensors, data acquisition systems, etc. for the real-time monitoring of the system. The real performance of the hybrid CAES system and the mathematical model's assumptions can be then quantified and validated. This includes quantifying the pressure and temperature losses throughout the system components under real-time operation. Therefore, this work provides a framework to further optimize the hybrid CAES system and investigate the potentials of different storage materials in the TES system. Also, the proposed ESS can be used to provide both electrical power and hot water. Therefore, investigating the cogeneration and trigeneration potentials of this hybrid system should be considered in the future research. Moreover, the proposed control strategy can be verified experimentally and optimized for further improvement of the ESS performance. Furthermore, investigation of different strategies for the energy management of hybrid CAES-TES systems can be conducted.

Besides, a more comprehensive environmental and economic analysis can be performed for the full system of the novel PFPV integrated with the proposed hybrid CAES system. This is to investigate the emissions saving resulting from the increase in output power and electrical efficiency resulting from the PV system's partial floating as well as the emissions saving by the proposed hybrid CAES system due to its independence from fossil fuel. Also, an economic optimization and analysis based on the levelized cost of energy measure are required for the full system at different submergence ratios and operational scenarios.

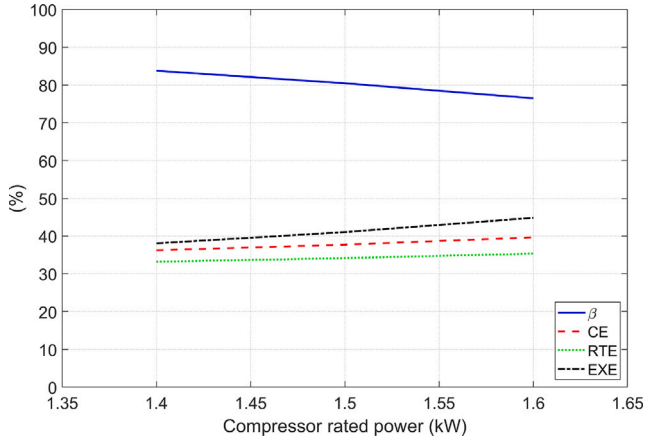

Fig. 19. System power distribution ratio and efficiency at different rated powers of the compressors.

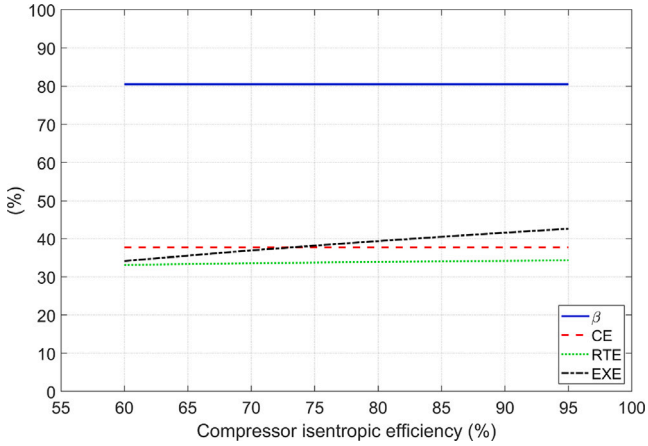

Fig. 20. System power distribution ratio and efficiency at different compressor's isentropic efficiency.

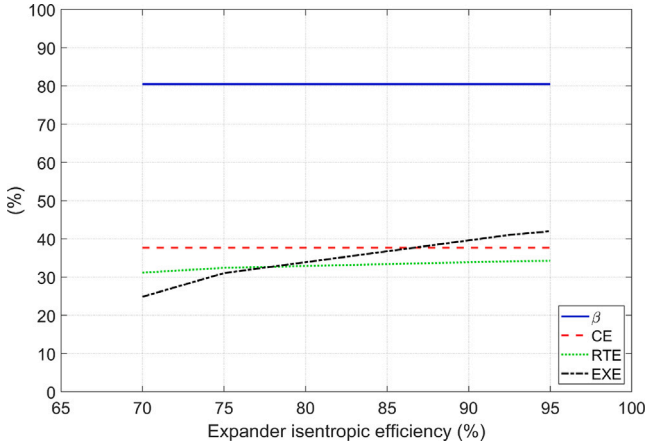

Fig. 21. System power distribution ratio and efficiency at different expander's isentropic efficiency.

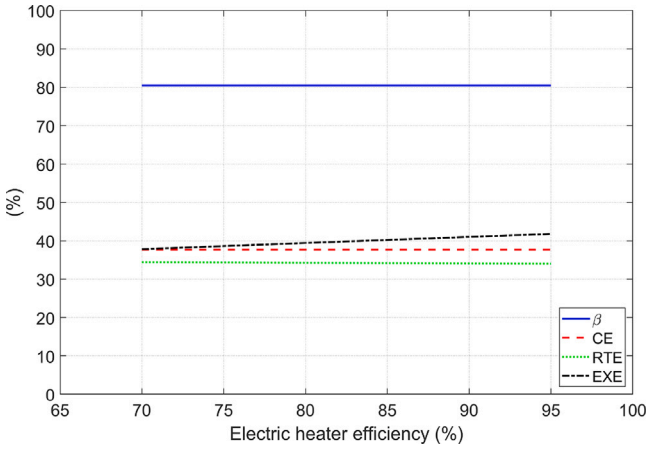

Fig. 22. System power distribution ratio and efficiency at different electric heater efficiency.

CRediT authorship contribution statement

Ameen M. Bassam: Writing – original draft, Visualization, Investigation, Conceptualization. **Nabil A.S. Elminshawy:** Writing – review & editing, Methodology, Investigation, Conceptualization. **Erkan Oterkus:** Writing – review & editing, Methodology, Conceptualization. **Islam Amin:** Writing – review & editing, Methodology, Conceptualization.

Declaration of competing interest

The authors declare that they have no known competing financial interests or personal relationships that could have appeared to influence the work reported in this paper.

Acknowledgments

This work was supported by a Institutional Links grant, ID 527194321, under the Egypt-Newton-Mosharafa Fund partnership. The grant is funded by the UK Department for Business, Energy and Industrial Strategy and Science, Technology and Innovation Funding Authority (STIFA) - project NO. 42715 (A Novel Partially Floating Photovoltaic Integrated with Smart Energy Storage and Management System for Egyptian Lakes) and delivered by the British Council.

Data availability

Data will be made available on request.

References

[1] Ahmad T, Zhang D. A critical review of comparative global historical energy consumption and future demand: The story told so far. Energy Rep 2020;6:1973–91.
[2] Bogdanov D, Ram M, Aghahosseini A, Gulagi A, Oyewo AS, Child M, et al. Low-cost renewable electricity as the key driver of the global energy transition towards sustainability. Energy 2021;227:120467.
[3] Salah SI, Eltaweel M, Abeykoon C. Towards a sustainable energy future for Egypt: A systematic review of renewable energy sources, technologies, challenges, and recommendations. Clean Eng Technol 2022;100497.
[4] El-Megharbel N. Sustainable development strategy: Egypt's vision 2030 and planning reform. Egypt: Ministry of Planning; 2015.
[5] Moharram NA, Tarek A, Gaber M, Bayoumi S. Brief review on Egypt's renewable energy current status and future vision. Energy Rep 2022;8:165–72.
[6] Sahu A, Yadav N, Sudhakar K. Floating photovoltaic power plant: A review. Renew Sustain Energy Rev 2016;66:815–24.

[7] Dwivedi P, Sudhakar K, Soni A, Solomin E, Kirpichnikova I. Advanced cooling techniques of PV modules: A state of art. Case Stud Therm Eng 2020;21:100674.
[8] Bassam AM, Amin I, Mohamed A, Elminshawy NA, Soliman HY, Elhenawy Y, et al. Conceptual design of a novel partially floating photovoltaic integrated with smart energy storage and management system for Egyptian North Lakes. Ocean Eng 2023;114416.
[9] Elminshawy NA, Mohamed A, Osama A, Amin I, Bassam AM, Oterkus E. Performance and potential of a novel floating photovoltaic system in Egyptian winter climate on calm water surface. Int J Hydrog Energy 2022;47(25):12798–814.
[10] Rahman MM, Oni AO, Gemechu E, Kumar A. Assessment of energy storage technologies: A review. Energy Convers Manage 2020;223:113295.
[11] Akbari H, Browne MC, Ortega A, Huang MJ, Hewitt NJ, Norton B, et al. Efficient energy storage technologies for photovoltaic systems. Sol Energy 2019;192:144–68.
[12] Cazzaniga R, Cicu M, Rosa-Clot M, Rosa-Clot P, Tina G, Ventura C. Floating photovoltaic plants: Performance analysis and design solutions. Renew Sustain Energy Rev 2018;81:1730–41.
[13] Olabi A, Wilberforce T, Ramadan M, Abdelkareem MA, Alami AH. Compressed air energy storage systems: Components and operating parameters–A review. J Energy Storage 2021;34:102000.
[14] Vollaro RDL, Faga F, Tallini A, Cedola L, Vallati A. Energy and thermodynamical study of a small innovative compressed air energy storage system (micro-CAES). Energy Procedia 2015;82:645–51.
[15] Razmi AR, Hanifi AR, Shahbakhti M. Design, thermodynamic, and economic analyses of a green hydrogen storage concept based on solid oxide electrolyzer/fuel cells and heliostat solar field. Renew Energy 2023;215:118996.
[16] Razmi AR, Alirahmi SM, Nabat MH, Assareh E, Shahbakhti M. A green hydrogen energy storage concept based on parabolic trough collector and proton exchange membrane electrolyzer/fuel cell: thermodynamic and exergoeconomic analyses with multi-objective optimization. Int J Hydrog Energy 2022;47(62):26468–89.
[17] Alirahmi SM, Mousavi SB, Razmi AR, Ahmadi P. A comprehensive techno-economic analysis and multi-criteria optimization of a compressed air energy storage (CAES) hybridized with solar and desalination units. Energy Convers Manage 2021;236:114053.
[18] Alirahmi SM, Razmi AR, Arabkoohsar A. Comprehensive assessment and multi-objective optimization of a green concept based on a combination of hydrogen and compressed air energy storage (CAES) systems. Renew Sustain Energy Rev 2021;142:110850.
[19] Razmi AR, Soltani M, Ardehali A, Gharali K, Dusseault M, Nathwani J. Design, thermodynamic, and wind assessments of a compressed air energy storage (CAES) integrated with two adjacent wind farms: A case study at Abhar and Kahak sites, Iran. Energy 2021;221:119902.
[20] Bushehri MC, Zolfaghari SM, Soltani M, Nabat MH, Nathwani J. A comprehensive study of a green hybrid multi-generation compressed air energy storage (CAES) system for sustainable cities: Energy, exergy, economic, exergoeconomic, and advanced exergy analysis. Sustainable Cities Soc 2024;101:105078.
[21] Assareh E, Ghafouri A. An innovative compressed air energy storage (CAES) using hydrogen energy integrated with geothermal and solar energy technologies: a comprehensive techno-economic analysis-different climate areas-using artificial intelligent (AI). Int J Hydrog Energy 2023;48(34):12600–21.
[22] Sheng L, Zhou Z, Charpentier J-F, Benbouzid M. Stand-alone island daily power management using a tidal turbine farm and an ocean compressed air energy storage system. Renew Energy 2017;103:286–94.
[23] Ma S, Wang X, Negnevitsky M, Franklin E. Performance investigation of a wave-driven compressed air energy storage system. J Energy Storage 2023;73:109126.
[24] Razmi AR, Afshar HH, Pourahmadiyan A, Torabi M. Investigation of a combined heat and power (CHP) system based on biomass and compressed air energy storage (CAES). Sustain Energy Technol Assess 2021;46:101253.
[25] Xue X, Lv J, Chen H, Xu G, Li Q. Thermodynamic and economic analyses of a new compressed air energy storage system incorporated with a waste-to-energy plant and a biogas power plant. Energy 2022;261:125367.
[26] Li Y, Cao H, Wang S, Jin Y, Li D, Wang X, et al. Load shifting of nuclear power plants using cryogenic energy storage technology. Appl Energy 2014;113:1710–6.
[27] Roushenas R, Razmi AR, Soltani M, Torabi M, Dusseault MB, Nathwani J. Thermo-environmental analysis of a novel cogeneration system based on solid oxide fuel cell (SOFC) and compressed air energy storage (CAES) coupled with turbocharger. Appl Therm Eng 2020;181:115978.
[28] Chen L, Zhang L, Wang Y, Xie M, Yang H, Ye K, et al. Design and performance evaluation of a novel system integrating water-based carbon capture with adiabatic compressed air energy storage. Energy Convers Manage 2023;276:116583.
[29] Budt M, Wolf D, Span R, Yan J. A review on compressed air energy storage: Basic principles, past milestones and recent developments. Appl Energy 2016;170:250–68.
[30] He W, Wang J. Optimal selection of air expansion machine in Compressed Air Energy Storage: A review. Renew Sustain Energy Rev 2018;87:77–95.
[31] Luo X, Dooner M, He W, Wang J, Li Y, Li D, et al. Feasibility study of a simulation software tool development for dynamic modelling and transient control of adiabatic compressed air energy storage with its electrical power system applications. Appl Energy 2018;228:1198–219.
[32] Houssainy S, Janbozorgi M, Ip P, Kavehpour P. Thermodynamic analysis of a high temperature hybrid compressed air energy storage (HTH-CAES) system. Renew Energy 2018;115:1043–54.
[33] Barbour ER, Pottie DL, Eames P. Why is adiabatic compressed air energy storage yet to become a viable energy storage option? IScience 2021;24(5):102440.
[34] Guo H, Xu Y, Zhu Y, Chen H, Lin X. Unsteady characteristics of compressed air energy storage systems with thermal storage from thermodynamic perspective. Energy 2022;244:122969.
[35] Nojavan S, Akbari-Dibavar A, Zare K. Optimal energy management of compressed air energy storage in day-ahead and real-time energy markets. IET Gener Transm Distrib 2019;13(16):3673–9.
[36] Lund H, Salgi G, Elmegaard B, Andersen AN. Optimal operation strategies of compressed air energy storage (CAES) on electricity spot markets with fluctuating prices. Appl Therm Eng 2009;29(5–6):799–806.
[37] Tong S, Cheng Z, Cong F, Tong Z, Zhang Y. Developing a grid-connected power optimization strategy for the integration of wind power with low-temperature adiabatic compressed air energy storage. Renew Energy 2018;125:73–86.
[38] Gao J, Chen J, Qi B, Zhao Y, Peng K, Zhang X. A cost-effective two-stage optimization model for microgrid planning and scheduling with compressed air energy storage and preventive maintenance. Int J Electr Power Energy Syst 2021;125:106547.
[39] Ghadi MJ, Azizivahed A, Mishra DK, Li L, Zhang J, Shafie-khah M, et al. Application of small-scale compressed air energy storage in the daily operation of an active distribution system. Energy 2021;231:120961.
[40] Marano V, Rizzo G, Tiano FA. Application of dynamic programming to the optimal management of a hybrid power plant with wind turbines, photovoltaic panels and compressed air energy storage. Appl Energy 2012;97:849–59.
[41] Li P, Yang C, Sun L, Xiang J, Wen X, Zhong J, et al. Dynamic characteristics and operation strategy of the discharge process in compressed air energy storage systems for applications in power systems. Int J Energy Res 2020;44(8):6363–82.
[42] Bai J, Liu F, Xue X, Wei W, Chen L, Wang G, et al. Modelling and control of advanced adiabatic compressed air energy storage under power tracking mode considering off-design generating conditions. Energy 2021;218:119525.
[43] Han Z, Guo S. Investigation of discharge characteristics of a tri-generative system based on advanced adiabatic compressed air energy storage. Energy Convers Manage 2018;176:110–22.
[44] Han Z, Guo S. Investigation of operation strategy of combined cooling, heating and power (CCHP) system based on advanced adiabatic compressed air energy storage. Energy 2018;160:290–308.
[45] Zhang X, Li Y, Gao Z, Chen S, Xu Y, Chen H. Overview of dynamic operation strategies for advanced compressed air energy storage. J Energy Storage 2023;66:107408.
[46] Jiang R, Qin FG, Chen B, Yang X, Yin H, Xu Y. Thermodynamic performance analysis, assessment and comparison of an advanced trigenerative compressed air energy storage system under different operation strategies. Energy 2019;186:115862.
[47] Guo H, Xu Y, Zhang X, Liang Q, Wang S, Chen H. Dynamic characteristics and control of supercritical compressed air energy storage systems. Appl Energy 2021;283:116294.
[48] He Q, Li G, Lu C, Du D, Liu W. A compressed air energy storage system with variable pressure ratio and its operation control. Energy 2019;169:881–94.
[49] Koçak B, Fernandez AI, Paksoy H. Review on sensible thermal energy storage for industrial solar applications and sustainability aspects. Sol Energy 2020;209:135–69.
[50] Inal OB, Charpentier JF, Deniz C. Hybrid power and propulsion systems for ships: Current status and future challenges. Renew Sustain Energy Rev 2022;156:111965.
[51] Tie SF, Tan CW. A review of energy sources and energy management system in electric vehicles. Renew Sustain Energy Rev 2013;20:82–102.
[52] Mozayeni H, Wang X, Negnevitsky M. Dynamic analysis of a low-temperature Adiabatic Compressed Air Energy Storage system. J Clean Prod 2020;276:124323.
[53] Wang Z, Xiong W, Ting DSK, Carriveau R, Wang Z. Conventional and advanced exergy analyses of an underwater compressed air energy storage system. Appl Energy 2016;180:810–22.
[54] Wang Z, Ting DSK, Carriveau R, Xiong W, Wang Z. Design and thermodynamic analysis of a multi-level underwater compressed air energy storage system. J Energy Storage 2016;5:203–11.
[55] Proczka J, Muralidharan K, Villela D, Simmons J, Frantziskonis G. Guidelines for the pressure and efficient sizing of pressure vessels for compressed air energy storage. Energy Convers Manage 2013;65:597–605.
[56] Chen S, Arabkoohsar A, Zhu T, Nielsen MP. Development of a micro-compressed air energy storage system model based on experiments. Energy 2020;197:117152.
[57] Wang P, Zhao P, Xu W, Wang J, Dai Y. Performance analysis of a combined heat and compressed air energy storage system with packed bed unit and electrical heater. Appl Therm Eng 2019;162:114321.
[58] Hoffeins H. Huntorf air storage gas turbine power plant. In: Energy supply, vol. 90, Brown Boveri Publication DGK; 1994, p. 202.
[59] Jafarizadeh H, Soltani M, Nathwani J. Assessment of the Huntorf compressed air energy storage plant performance under enhanced modifications. Energy Convers Manage 2020;209:112662.

[60] Hartmann N, Vöhringer O, Kruck C, Eltrop L. Simulation and analysis of different adiabatic compressed air energy storage plant configurations. Appl Energy 2012;93:541–8.
[61] Dincer I. Comprehensive energy systems. Elsevier; 2018.
[62] Global Solar Atlas. https://globalsolaratlas.info/map?s=31.12783,33.261233,10&pv=hydro,180,25,5. [Accessed 14 August 2023].
[63] Xinghua Y, Jiazhen P, Jidai W, Jing S. Simulation and experimental research on energy conversion efficiency of scroll expander for micro-compressed air energy storage system. Int J Energy Res 2014;38(7):884–95.
[64] Cheayb M, Gallego MM, Tazerout M, Poncet S. Modelling and experimental validation of a small-scale trigenerative compressed air energy storage system. Appl Energy 2019;239:1371–84.
[65] Dib G, Haberschill P, Rullière R, Perroit Q, Davies S, Revellin R. Thermodynamic simulation of a micro advanced adiabatic compressed air energy storage for building application. Appl Energy 2020;260:114248.
[66] Wang S, Zhang X, Yang L, Zhou Y, Wang J. Experimental study of compressed air energy storage system with thermal energy storage. Energy 2016;103:182–91.
[67] Houssainy S, Janbozorgi M, Kavehpour P. Thermodynamic performance and cost optimization of a novel hybrid thermal-compressed air energy storage system design. J Energy Storage 2018;18:206–17.
[68] Bartnik R, Buryn Z, Hnydiuk-Stefan A. Comparative thermodynamic and economic analysis of a conventional gas-steam power plant with a modified gas-steam power plant. Energy Convers Manage 2023;293:117502.